

# 6

## The Diagnosis of Mid-Latitude Synoptic-Scale Vertical Motions

### Objectives

Regions of upward vertical motion are often associated with clouds and precipitation since rising air cools by expansion. This cooling increases the relative humidity of the air which can eventually lead to condensation and cloud formation. Regions of rising air are also often associated with mass divergence in an atmospheric column and, consequently, surface pressure falls and cyclogenesis. Regions of downward vertical motion are often cloud free as air dries and warms upon being compressed as it sinks to higher pressure. Mass convergence into an atmospheric column, characteristic of regions of downward vertical motion, results in surface pressure rises and surface anti-cyclogenesis. As a result of the fundamental nature of these relationships, it is not an exaggeration to say that determination of where, when, and to what degree the air is rising or sinking is of fundamental importance for accurately diagnosing the current weather or predicting its future state. In this chapter we will investigate a number of different methods for diagnosing synoptic-scale vertical motions in typical mid-latitude weather systems.

Some of these diagnostic methods will derive from careful consideration of the ageostrophic wind vector itself. Several others (the Sutcliffe development theorem as well as the traditional and  $\vec{Q}$ -vector forms of the quasi-geostrophic omega equation) will arise from simultaneously solving the quasi-geostrophic vorticity and thermodynamic energy equations for the vertical motion,  $\omega$ , and will make reference only to the instantaneous mass distribution. Taken together, the collection of diagnostics to be developed in this chapter will provide us with a formidable set of tools for understanding the synoptic-scale behavior of mid-latitude weather systems. We begin our investigation by considering the ageostrophic wind.

## 6.1 The Nature of the Ageostrophic Wind: Isolating the Acceleration Vector

Recall that the geostrophic wind is non-divergent on an  $f$  plane. In fact, under such conditions only departures from geostrophy contribute to horizontal divergence and, through the continuity of mass, to vertical motions as shown in (4.9). For this reason it is extremely important to examine means by which the ageostrophic motions in the mid-latitude atmosphere might be diagnosed. We begin with the frictionless equation of motion

$$\frac{d\vec{V}}{dt} = -f\hat{k} \times \vec{V} - \nabla\phi, \quad (6.1)$$

and take the vertical cross-product of this expression to obtain

$$\frac{\hat{k}}{f} \times \frac{d\vec{V}}{dt} = \frac{\hat{k}}{f} \times (-f\hat{k} \times \vec{V}) - \frac{\hat{k}}{f} \times \nabla\phi. \quad (6.2a)$$

The right hand rule dictates that  $\hat{k} \times \hat{k} \times \vec{A} = -\vec{A}$ , and  $\vec{V}_g = (\hat{k}/f) \times \nabla\phi$ , so

$$\frac{\hat{k}}{f} \times \frac{d\vec{V}}{dt} = \vec{V} - \vec{V}_g = \vec{V}_{ag}. \quad (6.2b)$$

The famous British meteorologist R. C. Sutcliffe<sup>1</sup> reasoned that surface pressure falls resulted from vertical differences in mass divergence in a column. Larger mass divergence aloft than at the surface resulted in surface pressure falls and vice versa for surface pressure rises. Such differences in divergence could be related to differential accelerations at the surface and aloft through application of (6.2b). Thus, Sutcliffe argued that isolation of the acceleration vector could give insights into the sense of the vertical motion in an atmospheric column. Before presenting the elegant theory of Sutcliffe (1939), let us endeavor to isolate the acceleration vector, and its ageostrophic consequences, in two rather simple cases. These cases correspond to the two broad classes of circumstances in which geostrophic balance is violated: the presence of along-flow speed change and curvature in the flow.

The canonical synoptic example of along-flow speed change is the isolated jet streak. Shown in Figure 6.1 is the isotach distribution associated with an isolated wind speed maximum at 300 hPa in the northern hemisphere. The dashed line drawn perpendicular to the jet axis divides the jet into the so-called entrance region to its left and the exit region to its right. A parcel of air located on the western edge of the entrance region (indicated by the solid circle in Figure 6.1) would quite obviously experience an acceleration in the direction of the flow at that location. Hence, the

<sup>1</sup> R. C. Sutcliffe (1904–1991) received his Ph.D. in statistics but found employment with the British Meteorological Office in 1927. He worked with the famous Tor Bergeron while in Malta where he opined that weather forecasting was scarcely worthy of description as a scientific activity. He was among the first, and greatest, atmospheric scientists to insist that weather forecasting and diagnosis should proceed from the equations of motion. This insistence led to what might be considered the first major breakthrough in modern synoptic-dynamic meteorology and his most famous contribution, ‘A contribution to the problem of development’ (Sutcliffe 1947).

## 6.1 THE NATURE OF THE AGEOSTROPHIC WIND

149

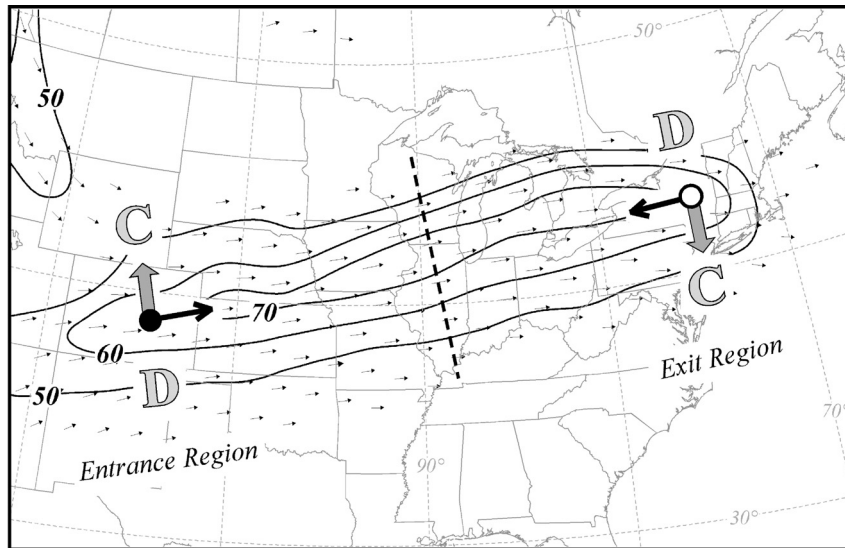


**Figure 6.1** The 300 hPa isotachs (solid lines) and wind vectors associated with a straight jet at 0000 UTC 12 November 2003 from NCEP's Eta model analysis. Isotachs are labeled in  $\text{m s}^{-1}$  and contoured every  $10 \text{ m s}^{-1}$  starting at  $50 \text{ m s}^{-1}$ . Only wind vectors greater than  $40 \text{ m s}^{-1}$  are shown. Thick black arrows indicate the direction of the acceleration vector  $d\vec{V}/dt$  at the entrance region (solid black circle) and exit regions (open circle) of the jet. The gray shaded arrow is the resultant ageostrophic wind vector,  $\vec{V}_{ag}$ , at both locations. C and D represent the locations of 300 hPa ageostrophic convergence and divergence, respectively

vector  $d\vec{V}/dt$  points eastward toward the center of the jet streak. Consequently, the ageostrophic wind vector,  $\vec{V}_{ag}$ , points northward at the indicated point. The result of this distribution of ageostrophic winds in the entrance region of the jet is that there is convergence of air at 300 hPa to the north of the indicated position and divergence of air at 300 hPa to the south of the indicated position. Given that 300 hPa is nearly at the top of the troposphere, upper-level divergence (convergence) is associated with upward (downward) vertical motion in the intervening column and so a thermally direct vertical circulation generally exists in the entrance region of a straight jet streak.

A parcel of air located on the eastern edge of the exit region (indicated by the open circle in Figure 6.1) would quite obviously experience a deceleration in the direction opposite the flow at that location. Hence, the vector  $d\vec{V}/dt$  points westward toward the center of the jet streak. Consequently, the ageostrophic wind vector,  $\vec{V}_{ag}$ , points southward at the indicated point. The result of this distribution of ageostrophic winds in the exit region of the jet is that there is convergence of air at 300 hPa to the south of the indicated position and divergence of air at 300 hPa to the north of the indicated position. Upward vertical motion occurs in the column beneath the upper divergence maxima and, thus, a thermally indirect vertical circulation generally exists in the exit region of a straight jet streak.

Curvature in the flow is also a circumstance that violates the geostrophic assumption. Consider flow through an upper tropospheric trough–ridge couplet where the

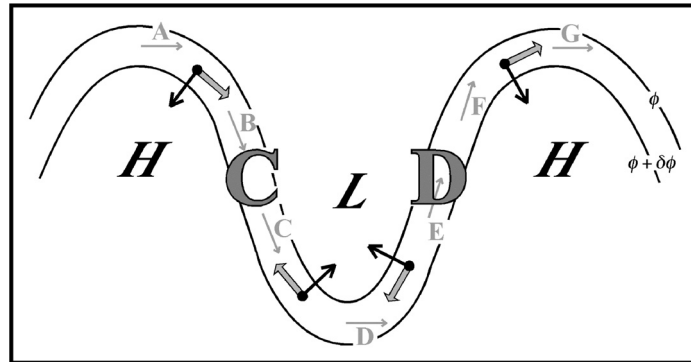


**Figure 6.2** Schematic upper tropospheric trough–ridge wave train in which the speed of the flow is the same everywhere. Thick black arrows represent the acceleration vectors,  $d\vec{V}/dt$ , at the indicated points determined graphically by finite differencing between adjacent wind arrows (in gray and labeled as described in the text). Gray shaded arrows represent resultant ageostrophic winds,  $\vec{V}_{ag}$ , at the indicated points. Convergence and divergence are indicated by C and D, respectively

wind speed is constant and everywhere parallel to the geopotential height lines as shown in Figure 6.2. Under such circumstances, the acceleration of the wind will be entirely a consequence of directional changes. Thus, between points A and B in Figure 6.2, a southwestward-directed acceleration is required to turn the wind from westerly at point A to northwesterly at point B. There is no direction change between points B and C and, thus, no acceleration vector. A northeastward-directed acceleration is required to turn the northwesterly wind at point C to a westerly direction at point D. In order to turn the westerly at point D to a southwesterly at point E, a northwestward-directed acceleration is required. No change in direction exists between points E and F but a change from southwesterly at F to westerly at point G requires a southeastward-directed acceleration as shown. Given the four acceleration vectors drawn in Figure 6.2, it is simple to draw the ageostrophic winds in this trough–ridge couplet. The ageostrophic winds clearly converge on the western side of the upper trough (on its upstream side) leading to downward vertical motion in the column in that location. Meanwhile, the divergence of the ageostrophic winds on the downstream side of the upper trough is associated with upward vertical motions in the column in that location. This result provides a first insight into the physical reason why inclement weather is often found downstream of upper-level trough axes while clear skies are often found downstream of upper-level ridge axes. This basic relationship lies at the heart of understanding the distribution of sensible weather in the middle latitudes.

### 6.1.1 Sutcliffe’s expression for net ageostrophic divergence in a column

Having examined the distribution of the ageostrophic winds in these canonical synoptic examples, let us now turn our attention to the insightful work of Sutcliffe

## 6.1 THE NATURE OF THE AGEOSTROPHIC WIND

151

(1939). We begin by considering the surface wind  $\vec{V}_0$ , the wind at some upper tropospheric level,  $\vec{V}$ , and the vertical shear between the two layers,  $\vec{V}_s$ . Based upon these simple definitions, it is clear that  $\vec{V} = \vec{V}_0 + \vec{V}_s$  and therefore

$$\frac{d\vec{V}}{dt} = \frac{d\vec{V}_0}{dt} + \frac{d\vec{V}_s}{dt} \quad (6.3)$$

where

$$\frac{d}{dt} = \frac{\partial}{\partial t} + \vec{V} \cdot \nabla$$

is the Lagrangian operator used to describe  $d\vec{V}/dt$ . Given these definitions, (6.3) can be expanded into

$$\frac{d\vec{V}}{dt} = \frac{\partial \vec{V}_0}{\partial t} + (\vec{V}_0 + \vec{V}_s) \cdot \nabla \vec{V}_0 + \frac{d\vec{V}_s}{dt}. \quad (6.4)$$

Alternatively, (6.4) can be written as

$$\frac{d\vec{V}}{dt} = \frac{\partial \vec{V}_0}{\partial t} + \vec{V}_0 \cdot \nabla \vec{V}_0 + \vec{V}_s \cdot \nabla \vec{V}_0 + \frac{d\vec{V}_s}{dt}. \quad (6.5)$$

Recognizing that the first two terms on the RHS of (6.5) describe the acceleration of the wind at the surface,  $(d\vec{V}/dt)_0$ , an expression for the differential acceleration in the layer arises:

$$\frac{d\vec{V}}{dt} - \left( \frac{d\vec{V}}{dt} \right)_0 = \vec{V}_s \cdot \nabla \vec{V}_0 + \frac{d\vec{V}_s}{dt}. \quad (6.6)$$

This expression relates the fact that if there is shearing over the surface wind ( $\vec{V}_s \cdot \nabla \vec{V}_0$ ) or a change in the shear vector ( $d\vec{V}_s/dt$ ) then there must be a difference in acceleration between the upper tropospheric wind and the surface wind. Based upon (6.2b), this implies that there must be some net divergence in the column and therefore, by continuity, vertical motions. Let us now examine the physical significance of the two terms on the RHS of (6.6). As we will do with every other diagnostic expression, we will consider the effect of each term in isolation, beginning with the shearing over the surface wind.

**(a) Shearing over the surface wind:**  $d\vec{V}/dt - (d\vec{V}/dt)_0 = \vec{V}_s \cdot \nabla \vec{V}_0$

Our expression begins by first expanding this term into its full component form given by

$$\vec{V}_s \cdot \nabla \vec{V}_0 = \left( u_s \frac{\partial u_0}{\partial x} + v_s \frac{\partial u_0}{\partial y} \right) \hat{i} + \left( u_s \frac{\partial v_0}{\partial x} + v_s \frac{\partial v_0}{\partial y} \right) \hat{j}. \quad (6.7)$$

Figure 6.3 depicts a schematic sea-level pressure minimum and some 1000–500 hPa thickness contours. Considering the value of this term at the center of the low-pressure

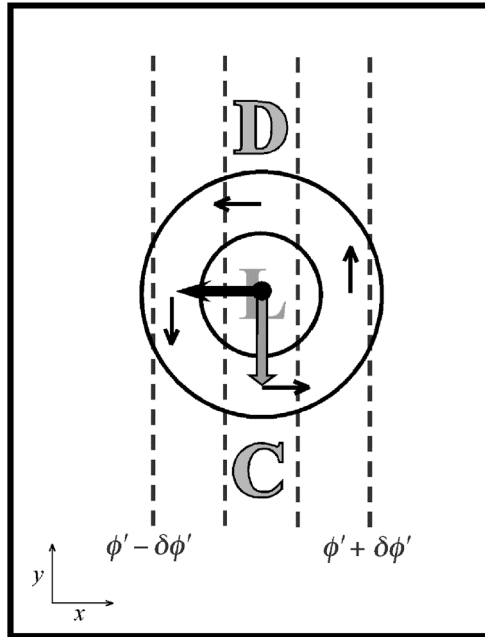


**Figure 6.3** Sea-level isobars (solid lines) and 1000–500 hPa thickness (dashed lines) near a developing surface low-pressure center in the northern hemisphere. Thin dark arrows represent the sea-level geostrophic winds. The thick black arrow represents  $\vec{V}_s \cdot \nabla \vec{V}_0$ . The gray shaded arrow represents the difference between the upper-level and surface ageostrophic wind,  $\vec{V}_{agU} - \vec{V}_{agL}$ . Net column convergence and divergence are indicated by C and D, respectively

center greatly reduces the mathematical complexity of applying (6.7). We will assume that the winds are geostrophic everywhere, which dictates that a thermal wind vector be directed along the positive  $y$ -axis in the northern hemisphere. At the center of the low, therefore, there is no  $x$ -direction vertical shear so that  $u_s = 0$ . It is also clear that there is no  $\partial v_0 / \partial y$  at the center of the low-pressure center. Thus, (6.7) reduces to

$$\vec{V}_s \cdot \nabla \vec{V}_0 = v_s \frac{\partial u_0}{\partial y} \hat{i}$$

for the scenario illustrated in Figure 6.3. We have already found that  $v_s$  is positive in this case. We now discern that  $\partial u_0 / \partial y$  is negative so that the product  $v_s \partial u_0 / \partial y$  is negative. Consequently, the vector  $\vec{V}_s \cdot \nabla \vec{V}_0$  points in the negative  $x$  direction as indicated. Since  $\vec{V}_s \cdot \nabla \vec{V}_0$  represents the acceleration at the top of the column minus the acceleration at the bottom of the column, taking the vertical cross-product of  $\vec{V}_s \cdot \nabla \vec{V}_0$  indicates the direction of the column-differential ageostrophic wind. Figure 6.3 shows that, in this case, there is greater ageostrophic divergence (convergence) aloft than at the surface north (south) of the surface low implying ascent (descent) in that location. The surface cyclone will propagate toward the net column mass divergence (i.e. in the direction of the ascending air) as only mass divergence and ascending air

6.1 THE NATURE OF THE AGEOSTROPHIC WIND

will be associated with sustained pressure falls at the surface. Application of similar reasoning to the case of a surface anticyclone (a recommended exercise for the reader) leads us to a general statement: *the sea-level pressure perturbation will propagate in the direction of the thermal wind.*

(b) Rate of change of the shear vector:  $d\vec{V}_s/dt$

Figure 6.4(a) shows some 1000–500 hPa thickness isopleths along with the thermal wind vector in the layer in the northern hemisphere at some time  $T = 0$ . Some time later ( $T = T_1$ ), the horizontal thickness gradient has been increased by some agency in the atmosphere such as confluent horizontal flow. The result of such an increase in the baroclinicity is a larger thermal wind, still directed to the north as shown in Figure 6.4(b). If we assume the winds are everywhere geostrophic, then the difference in the thermal wind vectors in Figures 6.4(a) and 6.4(b) represents a change in the shear vector and can be represented by the expression  $d\vec{V}_s/dt$  so long as the change has been measured following an individual air parcel. Thus,  $d\vec{V}_s/dt$  is directed in the positive  $y$  direction. The vertical cross-product of  $d\vec{V}_s/dt$  (which

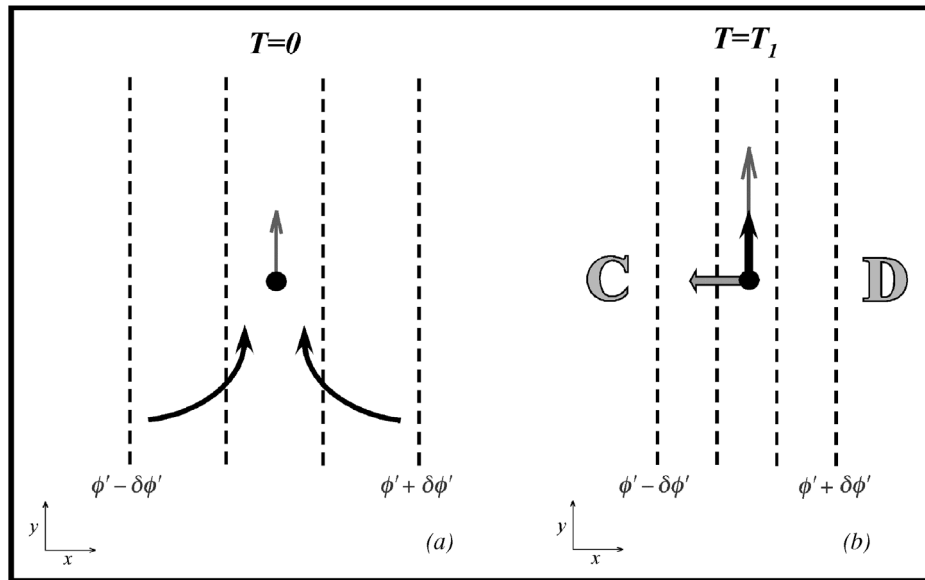


**Figure 6.4** Illustration of the effect of the rate of change of shear term,  $d\vec{V}_s/dt$ , from (6.6). Dashed lines are 1000–500 hPa thickness contours whose gradient increases in magnitude from time  $T = 0$  to time  $T = T_1$ . The increase is effected by horizontal confluence, represented by the thin black arrows in (a). The thin gray arrow represents  $\vec{V}_s$ , the thermal wind shear. At  $T = T_1$ , the thermal wind is larger and the bold black arrow in (b) represents the Lagrangian change in the shear,  $d\vec{V}_s/dt$ . The gray shaded arrow in (b) represents the difference between upper-level and near surface ageostrophic wind,  $\vec{V}_{agU} - \vec{V}_{agL}$ . Net column convergence and divergence are indicated by C and D, respectively

points directly toward the low thicknesses in Figure 6.4b) represents the column-differential ageostrophic wind for this example. The column of air on the warm (cold) side of the thickness gradient experiences greater divergence (convergence) aloft than at the surface and so it rises (sinks). Thus we find that anytime the horizontal flow acts to increase the thickness (or temperature) gradient, the response is the development of a thermally direct vertical circulation in which warm air rises and cold air sinks. Conversely, any systematic relaxation of the horizontal gradient of temperature by the action of the horizontal flow induces a thermally indirect vertical circulation. This physical insight, a direct consequence of the fact that the rate of change of the shear vector produces divergence in the column, is central to the dynamics of frontogenesis, a topic we will explore in great detail in Chapter 7.

### 6.1.2 Another perspective on the ageostrophic wind

We now turn our attention to a more formal expansion of the ageostrophic wind relationship (6.2b) which, recall, stated that

$$\vec{V}_{ag} = \frac{\hat{k}}{f} \times \frac{d\vec{V}}{dt}.$$

The Lagrangian derivative in the preceding expression can be expanded so that

$$\vec{V}_{ag} = \frac{\hat{k}}{f} \times \left( \frac{\partial \vec{V}}{\partial t} + \vec{V} \cdot \nabla \vec{V} + \omega \frac{\partial \vec{V}}{\partial p} \right). \quad (6.8)$$

The three terms on the RHS of (6.8) represent three contributions to the total ageostrophic wind: (1) the local wind tendency component, (2) the inertial advective component, and (3) the convective component. If we substitute  $\vec{V}_g$  for  $\vec{V}$  everywhere in (6.8) then

$$\vec{V}_{ag} = \frac{\hat{k}}{f} \times \left( \frac{\partial \vec{V}_g}{\partial t} + \vec{V}_g \cdot \nabla \vec{V}_g + \omega \frac{\partial \vec{V}_g}{\partial p} \right). \quad (6.9)$$

Our aim in this development is to diagnose the synoptic-scale vertical motion by first isolating the distribution of the ageostrophic wind. As is clear from (6.9), diagnosis of the convective component of the ageostrophic wind requires a priori knowledge of the vertical motion. Thus, it is not feasible to perform the intended diagnosis on the convective component. For this reason we will consider only the first two terms on the RHS of (6.9) in the foregoing analysis, starting with the local wind tendency component.

The local wind tendency component of the ageostrophic wind ( $\vec{V}_{agT}$ ) can be related to geopotential height or pressure changes since

$$\vec{V}_{agT} = \frac{\hat{k}}{f} \times \frac{\partial \vec{V}_g}{\partial t} = \frac{\hat{k}}{f} \times \frac{\partial}{\partial t} \left( \frac{\hat{k}}{f} \times \nabla \phi \right) = -\frac{1}{f^2} \nabla \frac{\partial \phi}{\partial t} \quad (6.10a)$$

## 6.1 THE NATURE OF THE AGEOSTROPHIC WIND

155

on pressure surfaces or

$$\frac{\hat{k}}{f} \times \frac{\partial \vec{V}_g}{\partial t} = -\frac{1}{\rho f^2} \nabla \frac{\partial p}{\partial t} \quad (6.10b)$$

on height surfaces. This component of the ageostrophic wind is known as the **isallobaric wind** as a result of its dependence on the gradient of isallobars (lines of constant pressure tendency,  $\partial p/\partial t$ ). Knowledge of the isallobaric wind, like any component of the ageostrophic wind, only tells us about the distribution of vertical motion when we know its divergence. Thus, we are most interested in the divergence of the isallobaric wind, given by

$$\nabla \cdot \vec{V}_{isal} = -\frac{1}{f^2} \nabla^2 \frac{\partial \phi}{\partial t} \quad (6.11a)$$

on pressure surfaces or

$$\nabla \cdot \vec{V}_{isal} = -\frac{1}{\rho f^2} \nabla^2 \frac{\partial p}{\partial t} \quad (6.11b)$$

on height surfaces. It is left as an exercise to show that pressure (or geopotential) falls are associated with convergence of the isallobaric wind while pressure (or geopotential) rises are associated with divergence of the isallobaric wind.

The inertial–advective component ( $\vec{V}_{IA}$ ) of the ageostrophic wind is given by

$$\vec{V}_{IA} = \frac{\hat{k}}{f} \times \left[ \left( u_g \frac{\partial u_g}{\partial x} + v_g \frac{\partial u_g}{\partial y} \right) \hat{i} + \left( u_g \frac{\partial v_g}{\partial x} + v_g \frac{\partial v_g}{\partial y} \right) \hat{j} \right]. \quad (6.12)$$

A number of different cases can be used to illustrate the effect of this term. Here we will examine two starting with the case of upper tropospheric diffluent flow illustrated in Figure 6.5(a). At the point in question, the expression in (6.12) is considerably simplified by the fact that the value of  $v_g$  at the point is identically zero. Additionally, there is no value of  $\partial v_g/\partial x$  there. Thus, the expression (6.12) reduces to

$$\vec{V}_{IA} = \frac{\hat{k}}{f} \times u_g \frac{\partial u_g}{\partial x} \hat{i}.$$

Noting that  $u_g > 0$  and  $\partial u_g/\partial x < 0$  at the indicated point,  $u_g \partial u_g/\partial x$  points in the negative  $x$  direction. Thus, the inertial advective wind,  $\vec{V}_{IA}$ , points in the negative  $y$  direction as indicated in Figure 6.5(a). As a consequence, there is upper-level divergence to the north of the indicated point and upper-level convergence to the south of it. Thus, the air will rise in the column to the north and sink in the column to the south. This pattern is precisely the same thermally indirect vertical circulation at the jet exit region that we diagnosed earlier.

We can also employ (6.12) to consider the effect of flow curvature on ageostrophy and vertical motions. A northern hemispheric 500 hPa ridge is shown schematically in Figure 6.5(b). If we imagine a case in which the magnitude of the geostrophic flow does not vary across the indicated points, then considerable simplification of (6.12) results. At the central point in Figure 6.5(b) it is clear that there is no value of  $v_g$ .

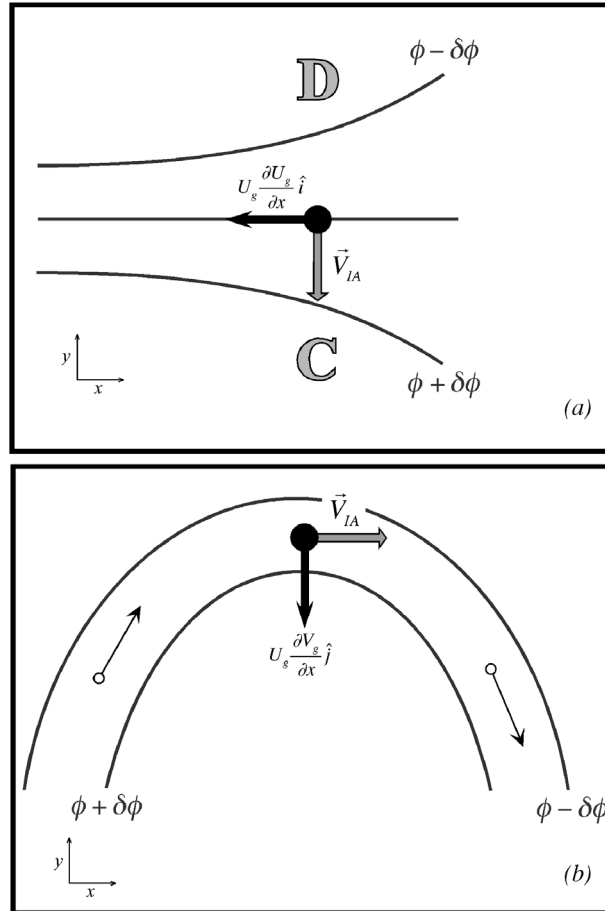


**Figure 6.5** (a) Inertial advective wind,  $\vec{V}_{IA}$ , in diffluent horizontal flow in the northern hemisphere. Solid lines are geopotential height at some upper tropospheric level (such as 300 hPa). Arrows are labeled as described in the text. Upper-level convergence and divergence of the inertial advective wind are represented by C and D, respectively. (b) Inertial advective wind through an upper-level ridge axis in the northern hemisphere. Lines labeled as in (a). Thin arrows represent the geostrophic flow through the ridge. See text for explanation

There is also no value for the derivative  $\partial u_g / \partial x$  at that point. Thus, (6.12) reduces to

$$\vec{V}_{IA} = \frac{\hat{k}}{f} \times u_g \frac{\partial v_g}{\partial x} \hat{j}$$

for the situation illustrated in Figure 6.5(b). At the crest of the ridge  $u_g$  is positive and  $\partial v_g / \partial x$  is negative so that  $u_g \partial v_g / \partial x$  points in the negative  $y$  direction. Consequently, the inertial advective wind,  $\vec{V}_{IA}$ , points in the direction of the geostrophic flow through the ridge. This analysis has demonstrated the familiar fact that the flow through a ridge axis is supergeostrophic and that this circumstance arises as

a result of the inertial advective component of the ageostrophic wind. The reader should consider the arguments made for confluent and cyclonically curved flow, respectively. Now that we have spent a good deal of effort considering vertical motions that arise from the divergence of the ageostrophic wind (i.e.  $\nabla \cdot (\hat{k}/f \times d\vec{V}/dt)$ ) we will move toward a related expression first derived by Sutcliffe in 1947.

### 6.2 The Sutcliffe Development Theorem

Sutcliffe made a refinement to his earlier theory (1939) by adopting the geostrophic assumption. Starting with the vector identity  $\vec{A} \cdot \vec{B} \times \vec{C} = -\vec{B} \cdot \vec{A} \times \vec{C}$ , Sutcliffe reasoned that the divergence of the ageostrophic wind was closely related to changes in the vertical component of vorticity. In mathematical terms,

$$-\nabla \cdot \hat{k} \times \frac{d\vec{V}}{dt} = \hat{k} \cdot \nabla \times \frac{d\vec{V}}{dt}. \tag{6.13}$$

Using the frictionless equations of motion in the  $x$  and  $y$  directions, the RHS of (6.13) becomes

$$\frac{\partial}{\partial x} \left( \frac{dv}{dt} = -\frac{\partial\phi}{\partial y} - fu \right) - \frac{\partial}{\partial y} \left( \frac{du}{dt} = -\frac{\partial\phi}{\partial x} + fv \right) \tag{6.14}$$

Letting

$$\frac{d}{dt} = \frac{\partial}{\partial t} + u\frac{\partial}{\partial x} + v\frac{\partial}{\partial y}, \quad \zeta = \frac{\partial v}{\partial x} - \frac{\partial u}{\partial y}, \quad \text{and} \quad \eta = \zeta + f,$$

(6.14) is a form of the vorticity equation<sup>2</sup>

$$\frac{d\eta}{dt} = \frac{d(\zeta + f)}{dt} = -(\zeta + f)\nabla \cdot \vec{V} \tag{6.15}$$

showing that vorticity changes are a result of divergence in the fluid. Next, Sutcliffe expanded this expression into its components

$$\frac{\partial(\zeta + f)}{\partial t} + \vec{V} \cdot \nabla(\zeta + f) + \omega \frac{\partial(\zeta + f)}{\partial p} = -(\zeta + f)\nabla \cdot \vec{V} \tag{6.16}$$

and assumed that (1) the vorticity and horizontal winds are geostrophic, (2) the vertical advection of vorticity is negligible, and (3) the relative vorticity can be neglected in the divergence term.<sup>3</sup> This yielded a simplified form of (6.16)

$$\frac{\partial(\zeta_g + f)}{\partial t} + \vec{V}_g \cdot \nabla(\zeta_g + f) = -f_0 \nabla \cdot \vec{V} \tag{6.17a}$$

<sup>2</sup> It is derived in the manner of (5.36) but since we have neglected vertical advection ( $\omega \partial/\partial p$ ) in the expression for the Lagrangian derivative, (6.15) contains no tilting term.

<sup>3</sup> These assumptions are precisely those that led to the quasi-geostrophic vorticity equation (5.43).

which can be rewritten as

$$\frac{1}{f} \nabla^2 \frac{\partial \phi}{\partial t} + \vec{V}_g \cdot \nabla (\zeta_g + f) = -f_0 \nabla \cdot \vec{V} \quad (6.17b)$$

since  $\zeta_g = (1/f) \nabla^2 \phi$ . Now if we consider the differences in divergence between the top and bottom of an air column, we can rewrite (6.17b) as

$$f_0 (\nabla \cdot \vec{V} - \nabla \cdot \vec{V}_0) = -\vec{V}_g \cdot \nabla (\zeta_g + f) + \vec{V}_{g_0} \cdot \nabla (\zeta_{g_0} + f) - \frac{1}{f} \nabla^2 \frac{\partial \phi'}{\partial t} \quad (6.18)$$

where

$$\frac{\partial \phi'}{\partial t} = \frac{\partial \phi}{\partial t} - \frac{\partial \phi_0}{\partial t}$$

represents the rate of change of thickness in the column. Thus, (6.18) demonstrates that vertical motion is related to (1) the change in the vertical distribution of vorticity by advection, and (2) the Laplacian of variation in the temperature field.

Considering the thickness tendency term first we find that since

$$\frac{\partial \phi'}{\partial t} = \underbrace{\frac{d\phi'}{dt}}_A - \underbrace{\vec{V} \cdot \nabla \phi'}_B - \underbrace{\omega \frac{\partial \phi'}{\partial p}}_C$$

there are three physical processes that can lead to a local change in thickness: (1) diabatic heating (A), (2) horizontal advection (B), and (3) vertical advection (adiabatic temperature changes) (C). If only diabatic heating were acting in the column, then  $\partial \phi' / \partial t > 0$  so that  $-\nabla^2 (\partial \phi' / \partial t) > 0$  and upward vertical motion would result according to (6.18). Conversely, diabatic cooling is associated with downward vertical motion. Adiabatic effects result from the very vertical motions we are trying to diagnose so the vertical advection term is difficult to interpret in this simplified framework and will therefore be neglected as it was in the vorticity equation (6.17a).

Let us consider horizontal advection as a means of producing the local thickness tendency. In such a case, the last term on the RHS of (6.18) could be written as

$$-\frac{1}{f} \nabla^2 \frac{\partial \phi'}{\partial t} = \frac{1}{f} \nabla^2 \left( \bar{u}_g \frac{\partial \phi'}{\partial x} + \bar{v}_g \frac{\partial \phi'}{\partial y} \right) \quad (6.19)$$

where the overbars denote column-averaged geostrophic winds. Substituting from the thermal wind equation ( $f v'_g = \partial \phi' / \partial x$  and  $-f u'_g = \partial \phi' / \partial y$ ) yields

$$-\frac{1}{f} \nabla^2 \frac{\partial \phi'}{\partial t} = \nabla^2 (\bar{u}_g v'_g - \bar{v}_g u'_g). \quad (6.20a)$$

## 6.2 THE SUTCLIFFE DEVELOPMENT THEOREM

159

This expression can be rearranged to yield

$$\begin{aligned}
& -\frac{1}{f}\nabla^2\frac{\partial\phi'}{\partial t} \\
& = \left(\bar{u}_g\frac{\partial}{\partial x} + \bar{v}_g\frac{\partial}{\partial y}\right)\left(\frac{\partial v'_g}{\partial x} - \frac{\partial u'_g}{\partial y}\right) + \left(\bar{u}_g\frac{\partial}{\partial y} - \bar{v}_g\frac{\partial}{\partial x}\right)\left(\frac{\partial u'_g}{\partial x} + \frac{\partial v'_g}{\partial y}\right) \\
& \quad - \left(u'_g\frac{\partial}{\partial x} + v'_g\frac{\partial}{\partial y}\right)\left(\frac{\partial\bar{v}_g}{\partial x} - \frac{\partial\bar{u}_g}{\partial y}\right) - \left(u'_g\frac{\partial}{\partial y} - v'_g\frac{\partial}{\partial x}\right)\left(\frac{\partial\bar{u}_g}{\partial x} + \frac{\partial\bar{v}_g}{\partial y}\right)
\end{aligned} \tag{6.20b}$$

so long as certain *products* of derivatives, i.e. terms such as

$$\frac{\partial\bar{u}_g}{\partial x}\frac{\partial v'_g}{\partial x},$$

are neglected.<sup>4</sup> Such terms are known as **deformation terms** and we will consider the consequences of their neglect later in this chapter. The second and fourth terms on the RHS of (6.20b) contain odd mixed derivatives of the divergence of the thermal wind (second term) and the divergence of the layer mean geostrophic wind (fourth term). Both of these quantities are zero and so (6.20b) can be further reduced to

$$-\frac{1}{f}\nabla^2\left(\frac{\partial\phi'}{\partial t}\right) = (\bar{\vec{V}}_g \cdot \nabla)\zeta'_g - (\vec{V}'_g \cdot \nabla)\bar{\zeta}_g. \tag{6.21}$$

Additional simplification arises by employing our definitions of the mean geostrophic wind in the layer ( $\bar{\vec{V}}_g = (\vec{V}_g + \vec{V}_{g0}/2)$ ), thermal wind in the layer ( $\vec{V}'_g = \vec{V}_g - \vec{V}_{g0}$ ), along with similar vertical average and vertical difference terms for the geostrophic vorticity ( $\bar{\zeta}_g = (\zeta_g + \zeta_{g0})/2$ ) and  $\zeta'_g = \zeta_g - \zeta_{g0}$ . In this case, (6.21) becomes

$$-\frac{1}{f}\nabla^2\left(\frac{\partial\phi'}{\partial t}\right) = \bar{\vec{V}}_{g0} \cdot \nabla\zeta_g - \vec{V}_g \cdot \nabla\zeta_{g0}. \tag{6.22}$$

This last expression describes only the contribution to net column divergence (via thickness tendencies) made by horizontal advection. So, we must substitute (6.22) into (6.18) to get

$$\begin{aligned}
f_0(\nabla \cdot \vec{V} - \nabla \cdot \vec{V}_0) & = -\bar{\vec{V}}_g \cdot \nabla(\zeta_g + f) + \bar{\vec{V}}_{g0} \cdot \nabla(\zeta_{g0} + f) \\
& \quad + \bar{\vec{V}}_{g0} \cdot \nabla\zeta_g - \vec{V}_g \cdot \nabla\zeta_{g0}.
\end{aligned}$$

<sup>4</sup> The full expansion of  $\nabla^2(\bar{u}_g v'_g)$ , for instance, involves expanding  $\partial^2(\bar{u}_g v'_g)/\partial x^2$  which, by the chain rule, is equal to

$$\frac{\partial}{\partial x}\left[\frac{\partial}{\partial x}(\bar{u}_g v'_g)\right] = \frac{\partial}{\partial x}\left[\bar{u}_g\frac{\partial v'_g}{\partial x} + v'_g\frac{\partial\bar{u}_g}{\partial x}\right] = \bar{u}_g\frac{\partial^2 v'_g}{\partial x^2} + 2\frac{\partial\bar{u}_g}{\partial x}\frac{\partial v'_g}{\partial x} + v'_g\frac{\partial^2\bar{u}_g}{\partial x^2}.$$

The first and third terms of this expression are found in (6.20b), but the product of derivatives term is not.

This expression can be reduced to

$$f_0(\nabla \cdot \vec{V} - \nabla \cdot \vec{V}_0) = -(\vec{V}_g - \vec{V}_{g_0}) \cdot \nabla(\zeta_{g_0} + \zeta_g + f),$$

or finally,

$$f_0(\nabla \cdot \vec{V} - \nabla \cdot \vec{V}_0) = -\vec{V}' \cdot \nabla(\zeta_{g_0} + \zeta_g + f) \quad (6.23)$$

which states that synoptic-scale upward (downward) vertical motions, the result of greater divergence (convergence) aloft than near the surface in any air column, are forced by cyclonic (anticyclonic) vorticity advection by the thermal wind! This is a remarkable result and represented one of the first operationally applicable theoretical results in the history of synoptic–dynamic meteorology. Consider the fact that given geopotential height analyses at two different isobaric levels, say 1000 and 500 hPa, it is easy to calculate graphically the distribution of thickness isopleths, parallel to which flows the thermal wind,  $\vec{V}'$ . Since  $\zeta_g = (1/f)\nabla^2\phi$ , it is equally simple to acquire a quick sense of the geostrophic vorticity at both levels. Thus, with just the geopotential height distribution at two levels, a theoretically solid basis for estimating the synoptic-scale vertical motion is offered by (6.23). Figure 6.6 illustrates the utility and ease of application of the Sutcliffe development theorem. Of course, the actual vertical motion distribution (Figure 6.6c) in any given storm is considerably more complicated than what might be expected from the Sutcliffe development term (Figure 6.6b) but the gross features are nicely captured by the simple approximated expression in (6.23).

### 6.3 The Quasi-Geostrophic Omega Equation

An alternative path to a diagnostic equation for synoptic-scale vertical motions arises from considering the quasi-geostrophic vorticity and thermodynamic energy equations. Recall that these expressions are given by

$$\frac{\partial \zeta_g}{\partial t} = -\vec{V}_g \cdot \nabla(\zeta_g + f) + f_0 \frac{\partial \omega}{\partial p} \quad (6.24a)$$

and

$$\frac{\partial}{\partial t} \left( -\frac{\partial \phi}{\partial p} \right) = -\vec{V}_g \cdot \nabla \left( -\frac{\partial \phi}{\partial p} \right) + \sigma \omega, \quad (6.25a)$$

respectively. Since the geostrophic relative vorticity can be expressed as the Laplacian of geopotential, this pair of equations can be rewritten as

$$\frac{1}{f_0} \nabla^2 \left( \frac{\partial \phi}{\partial t} \right) = -\vec{V}_g \cdot \nabla(\zeta_g + f) + f_0 \frac{\partial \omega}{\partial p} \quad (6.24b)$$

$$-\frac{\partial}{\partial p} \left( \frac{\partial \phi}{\partial t} \right) = -\vec{V}_g \cdot \nabla \left( -\frac{\partial \phi}{\partial p} \right) + \sigma \omega. \quad (6.25b)$$

6.3 THE QUASI-GEOSTROPHIC OMEGA EQUATION

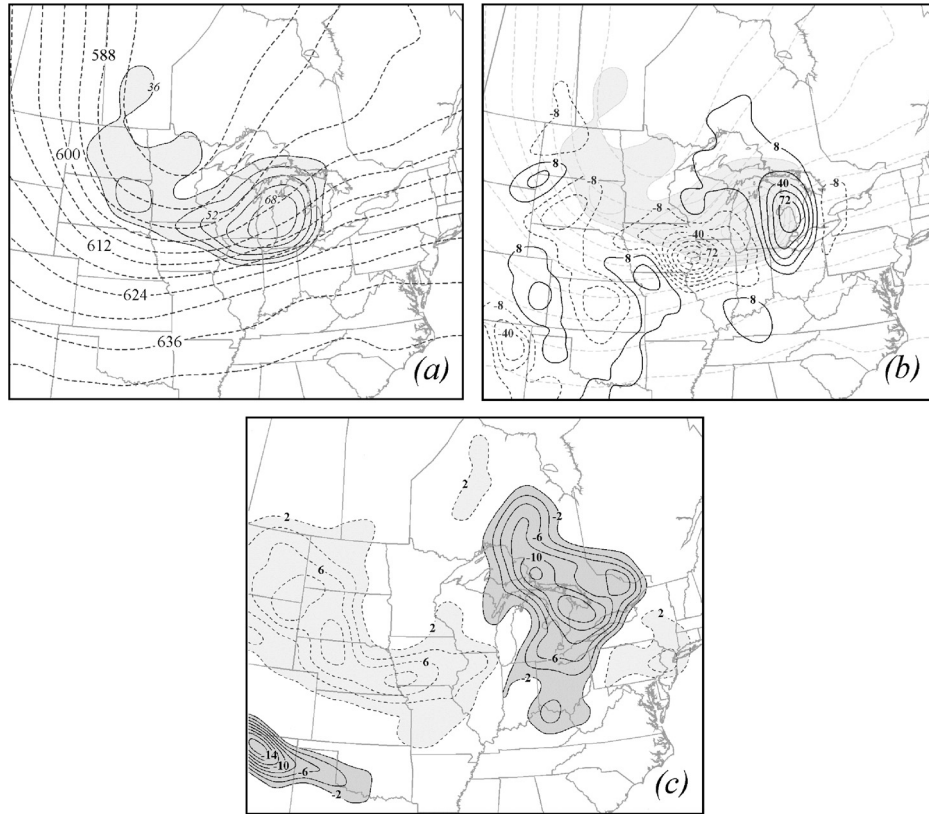


**Figure 6.6** (a) The 300–700 hPa thickness (dashed lines) and the sum  $\zeta_{g_{300}} + \zeta_{g_{700}} + f$  (shaded) at 0000 UTC 13 November 2003. Thickness is labeled in dam and contoured every 6 dam. Geostrophic vorticity is labeled in  $10^{-5} \text{ s}^{-1}$  and contoured every  $8 \times 10^{-5} \text{ s}^{-1}$  starting at  $36 \times 10^{-5} \text{ s}^{-1}$ . (b) Advection of the sum  $\zeta_{g_{300}} + \zeta_{g_{700}} + f$  by the 300–700 hPa thermal wind labeled in  $10^{-9} \text{ m kg}^{-1}$  and contoured every  $16 \times 10^{-9} \text{ m kg}^{-1}$  starting at  $8 \times 10^{-9} \text{ m kg}^{-1}$ . Vorticity and thickness from (a) are shown lightly in the background. (c) The 500 hPa vertical motion at 0000 UTC 13 November 2003. Vertical motion is labeled in  $\mu\text{bar s}^{-1}$  ( $\text{dPa s}^{-1}$ ) and contoured every  $2 \mu\text{bar s}^{-1}$  with dark (light) shading corresponding to upward (downward) vertical motion

In order to eliminate the time derivatives in both expressions, we take  $f_0 \partial/\partial p$  of (6.24b) and  $\nabla^2$  of (6.25b) to get

$$\frac{\partial}{\partial p} \nabla^2 \left( \frac{\partial \phi}{\partial t} \right) = f_0 \frac{\partial}{\partial p} [-\vec{V}_g \cdot \nabla (\zeta_g + f)] + f_0^2 \frac{\partial^2 \omega}{\partial p^2} \quad (6.24c)$$

$$-\frac{\partial}{\partial p} \nabla^2 \left( \frac{\partial \phi}{\partial t} \right) = \nabla^2 \left[ -\vec{V}_g \cdot \nabla \left( -\frac{\partial \phi}{\partial p} \right) \right] + \sigma \nabla^2 \omega. \quad (6.25c)$$

The sum of these two expressions yields

$$0 = f_0 \frac{\partial}{\partial p} [-\vec{V}_g \cdot \nabla (\zeta_g + f)] + f_0^2 \frac{\partial^2 \omega}{\partial p^2} + \nabla^2 \left[ -\vec{V}_g \cdot \nabla \left( -\frac{\partial \phi}{\partial p} \right) \right] + \sigma \nabla^2 \omega,$$

which can be rearranged into

$$\sigma \left( \nabla^2 + \frac{f_0^2}{\sigma} \frac{\partial^2}{\partial p^2} \right) \omega = f_0 \frac{\partial}{\partial p} [\vec{V}_g \cdot \nabla (\zeta_g + f)] + \nabla^2 \left[ \vec{V}_g \cdot \nabla \left( -\frac{\partial \phi}{\partial p} \right) \right], \quad (6.26)$$

known as the **quasi-geostrophic omega equation**. What does this expression mean? First, note that only derivatives in space exist in (6.26) so that it is a *diagnostic* equation for  $\omega$  in terms of the *instantaneous* geopotential height field. The value of such an expression is that we can obtain from it a measure of  $\omega$  that is not dependent on accurate observations of the wind. It is a rather complicated-looking expression so we will need to consider what physical meaning the mathematics contains.

The term on the LHS of (6.26), despite its complicated-looking nature, is essentially a 3-D Laplacian term. If we assume that the vertical motion field displays a sinusoidal vertical profile (which turns out to be a very solid assumption) then  $\partial^2 \omega / \partial p^2 \propto -\omega$ . Also, since the Laplacian is a second-derivative operator, a local maximum (minimum) in  $\nabla^2 \omega$  implies a local minimum (maximum) in  $\omega$  itself. Thus, whenever the RHS of (6.26) is found to be positive (negative), then  $\nabla^2 \omega$  is positive (negative) implying that  $\omega$  is negative (positive), corresponding to upward (downward) vertical motion.

The first term on the RHS of (6.26) physically represents the vertical derivative ( $-\partial/\partial p$ ) of geostrophic vorticity advection ( $-\vec{V}_g \cdot \nabla (\zeta_g + f)$ ). Thus, if an environment is characterized by geostrophic cyclonic vorticity advection increasing (decreasing) with height, then this term is positive (negative) implying that the environment will be characterized by upward (downward) vertical motion. Note the physical similarity between this term and the role of differential geostrophic vorticity advection in the Sutcliffe development theorem (6.18). Consider the schematic in Figure 6.7. Since geostrophic vorticity near the surface high and low is concentrated at those locations and the circulations are nearly closed at that level, the geostrophic vorticity advection near the surface is rather small. Geostrophic vorticity advection above the surface low, however, is large and positive so that that column experiences upward-increasing cyclonic vorticity advection and, hence, upward vertical motion. Geostrophic vorticity advection above the surface high is large and negative and that column experiences upward-decreasing cyclonic vorticity advection and, hence, downward vertical motion. It is important to note that since geostrophic vorticity is proportional to  $\nabla^2 \phi$  when the column above the surface low experiences a greater increase in geostrophic vorticity aloft than near the surface, this implies that

$$\frac{\partial}{\partial t} (\nabla^2 \phi - \nabla^2 \phi_0) > 0$$

or, alternatively,

$$\nabla^2 \frac{\partial \phi'}{\partial t} > 0$$

6.3 THE QUASI-GEOSTROPHIC OMEGA EQUATION

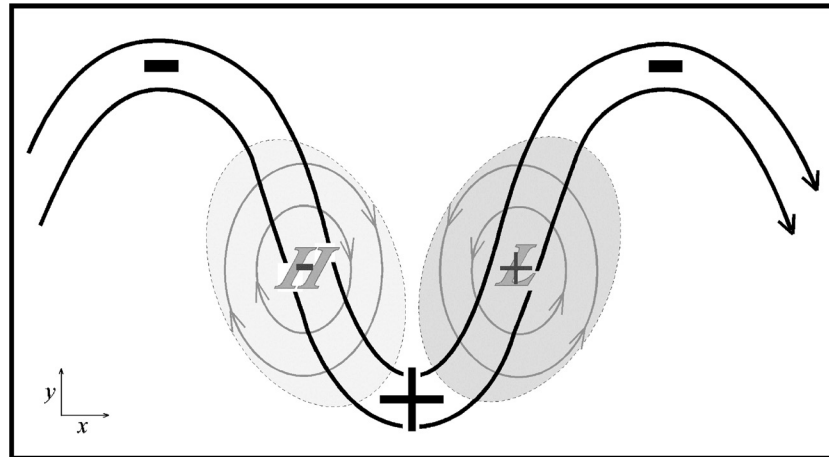


**Figure 6.7** The 500 hPa open wave over a surface low and surface high in the northern hemisphere. Thin gray lines are sea-level isobars with accompanying arrows indicating the direction of the near surface geostrophic flow. Thick black lines are the 500 hPa geopotential height with arrows indicating the direction of the 500 hPa geostrophic flow. The ‘+’ and ‘-’ represent the locations of positive and negative relative vorticities, respectively, with the size of the symbol indicating the relative magnitude of the vorticity (i.e. larger at upper levels). Dark (light) gray shaded ovals indicate regions of upward (downward) vertical motions. See text for explanation

which requires that

$$\frac{\partial \phi'}{\partial t} < 0.$$

In order to experience the requisite thickness decrease, the column must cool. The cooling is achieved by adiabatic expansion of the rising air.

The second term on the RHS of (6.26) can be rewritten as

$$\nabla^2 \left[ \vec{V}_g \cdot \nabla \left( -\frac{\partial \phi}{\partial p} \right) \right] = -\nabla^2 \left[ -\vec{V}_g \cdot \nabla \left( -\frac{\partial \phi}{\partial p} \right) \right].$$

This alternative form makes it clear that the term in the brackets physically represents horizontal temperature advection. Thus, this entire expression describes the Laplacian of horizontal temperature advection. If an environment is characterized by a *local* maximum in warm (cold) air advection, then this term is positive (negative), corresponding to upward (downward) vertical motion. It is important to note that, according to the quasi-geostrophic omega equation, warm (cold) air advection alone is not enough to diagnose the sense of the vertical motion – it is the Laplacian of the temperature advection that matters. This implies that *only heterogeneity in the thermal advection field is associated with  $\omega$* . This is easily demonstrated by considering an alternative form of this term:

$$-\nabla \cdot \nabla \left[ -\vec{V}_g \cdot \nabla \left( -\frac{\partial \phi}{\partial p} \right) \right].$$

It is clear that if the *gradient* of horizontal temperature advection is zero (i.e. there is uniform horizontal temperature advection) then the whole term will be zero and no vertical motion will be forced.

The vertical motion fields described by the quasi-geostrophic omega equation are precisely those vertical motions that are required to keep the thermal and mass fields in hydrostatic and geostrophic balance. These diagnosed vertical motions also tend to be an accurate description of the large-scale vertical motions observed in the mid-latitude atmosphere. We will investigate why vertical motions are required to maintain thermal wind balance presently. First, it is enlightening to examine a simplified form of (6.26) that renders a result similar to that described by the Sutcliffe development theorem.

Trenberth (1978) argued that carrying out all the derivatives on the RHS of (6.26) could simplify the forcing function of the quasi-geostrophic omega equation. Expanding the terms in square brackets on the RHS of (6.26) yields

$$\sigma \left( \nabla^2 + \frac{f_0^2}{\sigma} \frac{\partial^2}{\partial p^2} \right) \omega = f_0 \frac{\partial}{\partial p} \left[ u_g \frac{\partial(\zeta_g + f)}{\partial x} + v_g \frac{\partial(\zeta_g + f)}{\partial y} \right] + \nabla^2 \left[ -u_g \frac{\partial^2 \phi}{\partial x \partial p} - v_g \frac{\partial^2 \phi}{\partial y \partial p} \right]. \quad (6.27)$$

Employing the geostrophic wind relationships

$$u_g = -\frac{1}{f} \frac{\partial \phi}{\partial y} \quad \text{and} \quad v_g = \frac{1}{f} \frac{\partial \phi}{\partial x}$$

along with the definition of the geostrophic relative vorticity ( $\zeta_g = (1/f_0)\nabla^2\phi$ ) gives

$$\begin{aligned} & \sigma \left( \nabla^2 + \frac{f_0^2}{\sigma} \frac{\partial^2}{\partial p^2} \right) \omega \\ &= f_0 \frac{\partial}{\partial p} \left[ -\frac{1}{f} \frac{\partial \phi}{\partial y} \frac{\partial}{\partial x} \left( \frac{1}{f_0} \nabla^2 \phi + f \right) + \frac{1}{f} \frac{\partial \phi}{\partial x} \frac{\partial}{\partial y} \left( \frac{1}{f_0} \nabla^2 \phi + f \right) \right] \\ & \quad - \frac{1}{f} \nabla^2 \left[ -\frac{\partial \phi}{\partial y} \frac{\partial^2 \phi}{\partial x \partial p} + \frac{\partial \phi}{\partial x} \frac{\partial^2 \phi}{\partial y \partial p} \right]. \end{aligned} \quad (6.28)$$

Using the *Jacobian* operator,  $J(A, B)$ , where

$$J(A, B) = \left( \frac{\partial A}{\partial x} \frac{\partial B}{\partial y} - \frac{\partial A}{\partial y} \frac{\partial B}{\partial x} \right),$$

(6.28) can be rewritten as

$$\sigma \left( \nabla^2 + \frac{f_0^2}{\sigma} \frac{\partial^2}{\partial p^2} \right) \omega = \frac{1}{f} [F_1 + F_2]$$

## 6.3 THE QUASI-GEOSTROPHIC OMEGA EQUATION

165

where  $F_1$  and  $F_2$  are given by

$$F_1 = -J \left( \nabla^2 \phi, \frac{\partial \phi}{\partial p} \right) - J \left( \phi, \nabla^2 \frac{\partial \phi}{\partial p} \right) - 2 \left[ J \left( \frac{\partial \phi}{\partial x}, \frac{\partial^2 \phi}{\partial x \partial p} \right) + J \left( \frac{\partial \phi}{\partial y}, \frac{\partial^2 \phi}{\partial y \partial p} \right) \right] \quad (6.29)$$

$$F_2 = J \left( \frac{\partial \phi}{\partial p}, \nabla^2 \phi \right) + J \left( \frac{\partial \phi}{\partial p}, f f_0 \right) + J \left( \phi, \nabla^2 \frac{\partial \phi}{\partial p} \right), \quad (6.30)$$

respectively. Notice that the second term on the RHS of (6.29) is the additive inverse of the third term on the RHS of (6.30). Also,  $F_1$  contains the deformation terms (the square bracketed term on the RHS of (6.29)) which we neglected in the Sutcliffe development theorem. Upon neglecting them here again, we find that the RHS of (6.28) can be approximated as

$$\frac{1}{f} [F_1 + F_2] \approx \frac{1}{f} \left[ 2J \left( \frac{\partial \phi}{\partial p}, \nabla^2 \phi \right) + J \left( \frac{\partial \phi}{\partial p}, f f_0 \right) \right] \quad (6.31a)$$

which can be approximated further, without much error and to facilitate application, as

$$\frac{1}{f} [F_1 + F_2] \approx \frac{2}{f} \left[ J \left( \frac{\partial \phi}{\partial p}, \nabla^2 \phi \right) + J \left( \frac{\partial \phi}{\partial p}, f f_0 \right) \right]. \quad (6.31b)$$

Upon expansion of (6.31b), we find that an approximate form of the RHS of (6.26), the quasi-geostrophic omega equation, is given by

$$\sigma \left( \nabla^2 + \frac{f_0^2}{\sigma} \frac{\partial^2}{\partial p^2} \right) \omega \approx 2 \left[ f_0 \frac{\partial \vec{V}_g}{\partial p} \cdot \nabla (\zeta_g + f) \right]. \quad (6.32)$$

Thus, even when proceeding from the classical quasi-geostrophic omega equation, the fundamental physical insight achieved by Sutcliffe is confirmed: that is, large-scale mid-latitude vertical motions are forced by thermal wind advection of absolute geostrophic vorticity.

This result is both reassuring and convenient in the sense that it compresses a rather complicated expression (6.26) into a single forcing term that is easy to employ qualitatively using standard observations. Some nagging questions undoubtedly persist in the reader's mind at this point in our discussion, however. Perhaps chief among them is: *Is it reasonable that we continually neglect the so-called deformation terms in deriving diagnostic expressions for the large-scale, mid-latitude vertical motions?* Also, perhaps lurking deeper in the mind of the reader: *How do these quasi-geostrophic vertical motions serve to maintain the thermal wind balance?* Before we consider the second question, let us first consider the nature of the neglected deformation terms. The deformation terms appeared explicitly in (6.29) as

$$DEF = -\frac{2}{f} \left[ J \left( \frac{\partial \phi}{\partial x}, \frac{\partial^2 \phi}{\partial x \partial p} \right) + J \left( \frac{\partial \phi}{\partial y}, \frac{\partial^2 \phi}{\partial y \partial p} \right) \right]. \quad (6.33a)$$

Employing the geostrophic ( $f v_g = \partial\phi/\partial x$  and  $-f u_g = \partial\phi/\partial y$ ) and the hydrostatic ( $\partial\phi/\partial p = -RT/p$ ) relationships, this can be expressed as

$$DEF = -\frac{2}{f} \left[ J \left( f v_g, -\frac{R}{p} \frac{\partial T}{\partial x} \right) + J \left( -f u_g, -\frac{R}{p} \frac{\partial T}{\partial y} \right) \right]$$

or

$$DEF = \frac{2R}{p} \left[ J \left( v_g, \frac{\partial T}{\partial x} \right) - J \left( u_g, \frac{\partial T}{\partial y} \right) \right]. \quad (6.33b)$$

Carrying out the indicated derivatives and then grouping like terms together yields

$$DEF = \frac{2R}{p} \left[ \left( \frac{\partial v_g}{\partial x} + \frac{\partial u_g}{\partial y} \right) \frac{\partial^2 T}{\partial x \partial y} - \frac{\partial v_g}{\partial y} \frac{\partial^2 T}{\partial x^2} - \frac{\partial u_g}{\partial x} \frac{\partial^2 T}{\partial y^2} \right]. \quad (6.33c)$$

Denoting the geostrophic shearing deformation,  $(\partial v_g/\partial x + \partial u_g/\partial y)$ , as SH, the geostrophic stretching deformation,  $(\partial u_g/\partial x - \partial v_g/\partial y)$ , as ST, and employing the non-divergence of the geostrophic wind, (6.33c) can be rewritten as

$$DEF = \frac{2R}{P} \left[ (SH) \frac{\partial^2 T}{\partial x \partial y} + \frac{(ST)}{2} \left( \frac{\partial^2 T}{\partial x^2} - \frac{\partial^2 T}{\partial y^2} \right) \right] \quad (6.33d)$$

which illustrates that the deformation terms will be significant where second derivatives of temperature are coincident with deformation (i.e. first derivatives) in the geostrophic wind field. Mid-latitude frontal regions, as we will see, are defined by such conditions. This fact has led to the historical assumption that the deformation term is only large in frontal regions. As it turns out, a number of other recurrent but non-frontal thermal structures in mid-latitude cyclones are also characterized by these conditions – most notably the large-scale thermal ridge often associated with occluded cyclones. From this perspective, neglect of the deformation term is liable to lead to significant misdiagnosis in many canonical mid-latitude cyclone environments (as we will show later). Next we will derive an alternative expression for the forcing for quasi-geostrophic vertical motions that includes these terms, lends additional insight into the nature of the mid-latitude atmosphere, and is amenable to simple graphical evaluation.

## 6.4 The $\vec{Q}$ -Vector

The remainder of this chapter will be devoted to examining the so-called  $\vec{Q}$ -vector form of the quasi-geostrophic omega equation introduced by Hoskins *et al.* (1978). Consideration of the  $\vec{Q}$ -vector reveals an unexpected and intriguing characteristic of the thermal wind balance that will serve as a cornerstone in the development of a deeper conceptual understanding of the nature of quasi-geostrophic vertical motions. We begin by investigating the geostrophic paradox.

**6.4.1 The geostrophic paradox and its resolution**

Consider the jet entrance region depicted in Figure 6.8. The confluent, geostrophic wind field depicted there acts to tighten the horizontal temperature gradient at C. Any such increase in the magnitude of the temperature gradient forces an increase in the geostrophic vertical shear via the thermal wind relationship. Simultaneously, the geostrophic wind advects lower geostrophic momentum (quantified by the isotachs of the  $y$ -direction geostrophic wind) into the jet core. The momentum advection tends to decrease the wind speed at C and, thus, contributes to a decrease in the vertical shear of the geostrophic wind in that column. Thus, the very same geostrophic flow that serves to increase the magnitude of the horizontal temperature gradient at C also serves to decrease the vertical shear of the geostrophic wind at C via negative geostrophic momentum advection. This set of circumstances presents a paradox: that is, on the one hand, geostrophic temperature advection should increase the thermal wind at C and, on the other, geostrophic momentum advection should decrease it at C. So, the geostrophic wind actually destroys thermal wind balance by affecting opposite signed changes to the two components of that balance. Since the thermal wind balance is a form of the geostrophic balance, it can therefore be said that the geostrophic wind destroys itself! We will refer to this property of the geostrophic flow as the geostrophic paradox.

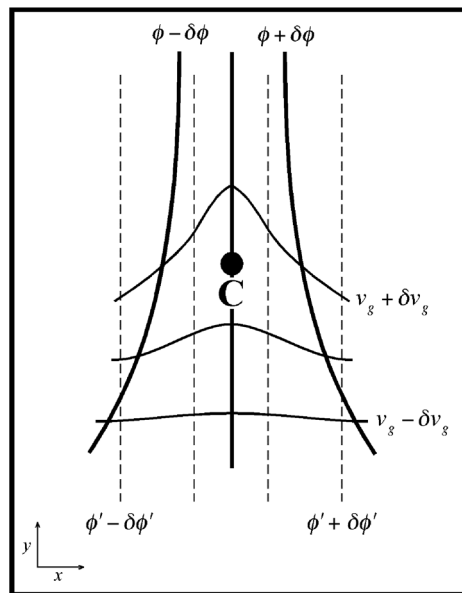


**Figure 6.8** Jet entrance region in the northern hemisphere. Thick solid lines are 500 hPa geopotential height, dashed lines are 1000–500 hPa thickness, and thin solid lines are isotachs of the  $y$ -direction geostrophic wind. Point C is mentioned in the explanation given in the text

Interestingly, however, observations suggest that the synoptic-scale flow in the middle latitudes is very nearly in geostrophic balance at all times. How can this be in the face of what we have just described? There must be another portion of the flow that acts to maintain the geostrophic balance in the face of its self-destructive tendency. That portion of the flow is the forced, ageostrophic, secondary circulation.<sup>5</sup> Since the geostrophic flow tends to create thermal wind imbalance, the forced secondary circulation must bring the flow back toward a state of geostrophic balance. This may be accomplished if the secondary circulation counteracts the tendencies induced by the geostrophic wind itself. Therefore, the secondary, ageostrophic circulation operating in the vicinity of the jet entrance region depicted in Figure 6.8 must simultaneously (1) decrease the magnitude of the horizontal temperature gradient, and (2) increase the vertical shear. We now examine a derivation that quantifies the geostrophic paradox and in so doing leads to a description of the forced, secondary circulation that resolves it.

We begin by considering both the thermodynamic energy equation and the  $y$  equation of motion at the level of quasi-geostrophic theory:

$$\left(\frac{\partial}{\partial t} + \vec{V}_g \cdot \nabla\right) v_g + f_0 u_{ag} = 0 \quad \text{and} \quad \left(\frac{\partial}{\partial t} + \vec{V}_g \cdot \nabla\right) \left(-\frac{\partial \phi}{\partial p}\right) - \sigma \omega = 0.$$

Neglecting the ageostrophy for the moment, these expressions can be rewritten as

$$\left(\frac{\partial}{\partial t} + \vec{V}_g \cdot \nabla\right) v_g = 0 \quad (6.34a)$$

and

$$\left(\frac{\partial}{\partial t} + \vec{V}_g \cdot \nabla\right) \left(-\frac{\partial \phi}{\partial p}\right) = 0. \quad (6.35a)$$

Recall that the thermal wind balance for the situation depicted in Figure 6.8 is given by

$$f_0 \frac{\partial v_g}{\partial p} = \frac{\partial^2 \phi}{\partial x \partial p}.$$

Now,  $f_0 \partial/\partial p$  of (6.34a) is equal to

$$\begin{aligned} f_0 \frac{\partial}{\partial p} \left[ \left(\frac{\partial}{\partial t} + \vec{V}_g \cdot \nabla\right) v_g \right] &= f_0 \frac{\partial}{\partial p} \left[ \frac{\partial v_g}{\partial t} + u_g \frac{\partial v_g}{\partial x} + v_g \frac{\partial v_g}{\partial y} \right] \\ &= \left(\frac{\partial}{\partial t} + \vec{V}_g \cdot \nabla\right) \left( f_0 \frac{\partial v_g}{\partial p} \right) \\ &\quad + f_0 \left[ \frac{\partial u_g}{\partial p} \frac{\partial v_g}{\partial x} + \frac{\partial v_g}{\partial p} \frac{\partial v_g}{\partial y} \right]. \end{aligned}$$

<sup>5</sup> This flow is referred to as 'secondary' in order to distinguish it from the primary, geostrophic flow.

6.4 THE  $\vec{Q}$ -VECTOR

169

Employing the thermal wind relationship and the non-divergence of the geostrophic wind, this can be rewritten as

$$f_0 \frac{\partial}{\partial p} \left[ \left( \frac{\partial}{\partial t} + \vec{V}_g \cdot \nabla \right) v_g \right] = \left( \frac{\partial}{\partial t} + \vec{V}_g \cdot \nabla \right) \left( f_0 \frac{\partial v_g}{\partial p} \right) + \left[ \frac{\partial \vec{V}_g}{\partial x} \cdot \nabla \left( -\frac{\partial \phi}{\partial p} \right) \right]. \quad (6.34b)$$

Interestingly,  $-\partial/\partial x$  of (6.35a) is equal to

$$\begin{aligned} & -\frac{\partial}{\partial x} \left[ \left( \frac{\partial}{\partial t} + \vec{V}_g \cdot \nabla \right) \left( -\frac{\partial \phi}{\partial p} \right) \right] \\ &= -\frac{\partial}{\partial x} \left[ \frac{\partial}{\partial t} \left( -\frac{\partial \phi}{\partial p} \right) + u_g \frac{\partial}{\partial x} \left( -\frac{\partial \phi}{\partial p} \right) + v_g \frac{\partial}{\partial y} \left( -\frac{\partial \phi}{\partial p} \right) \right] \\ &= \left( \frac{\partial}{\partial t} + \vec{V}_g \cdot \nabla \right) \left( \frac{\partial^2 \phi}{\partial x \partial p} \right) - \left[ \frac{\partial \vec{V}_g}{\partial x} \cdot \nabla \left( -\frac{\partial \phi}{\partial p} \right) \right]. \end{aligned} \quad (6.35b)$$

Examination of the last lines of (6.34b) and (6.35b) proves that the geostrophic tendencies of  $f_0 \partial v_g / \partial p$  and  $\partial^2 \phi / \partial x \partial p$  (the two components of the thermal wind balance) have equal magnitude but opposite sign! Thus, the geostrophic wind destroys itself by changing the two parts of the thermal wind balance equally, but in opposite directions. Let us denote the magnitude of this geostrophic tendency as  $Q_1$  so that

$$Q_1 = -\frac{\partial \vec{V}_g}{\partial x} \cdot \nabla \left( -\frac{\partial \phi}{\partial p} \right).$$

If we now reinsert the ageostrophic terms that we previously neglected in developing (6.34a) and (6.35a), we get

$$f_0 \frac{\partial}{\partial p} \left[ \left( \frac{\partial}{\partial t} + \vec{V}_g \cdot \nabla \right) v_g + f_0 u_{ag} \right] = \left( \frac{\partial}{\partial t} + \vec{V}_g \cdot \nabla \right) \left( f_0 \frac{\partial v_g}{\partial p} \right) - Q_1 + f_0^2 \frac{\partial u_{ag}}{\partial p} \quad (6.36)$$

and

$$-\frac{\partial}{\partial x} \left[ \left( \frac{\partial}{\partial t} + \vec{V}_g \cdot \nabla \right) \left( -\frac{\partial \phi}{\partial p} \right) - \sigma \omega \right] = \left( \frac{\partial}{\partial t} + \vec{V}_g \cdot \nabla \right) \left( \frac{\partial^2 \phi}{\partial x \partial p} \right) + Q_1 + \sigma \frac{\partial \omega}{\partial x}. \quad (6.37)$$

Multiplying (6.37) by  $-1$  and adding it to (6.36) eliminates the time derivatives (since  $f_0 \partial v_g / \partial p = \partial^2 \phi / \partial x \partial p$  by the thermal wind) and yields

$$-2Q_1 = \sigma \frac{\partial \omega}{\partial x} - f_0^2 \frac{\partial u_{ag}}{\partial p}. \quad (6.38)$$

The same set of operations can be performed on the  $x$  equation of motion and the thermodynamic energy equation resulting in

$$-2Q_2 = \sigma \frac{\partial \omega}{\partial y} - f_0^2 \frac{\partial v_{ag}}{\partial p} \quad (6.39)$$

where

$$Q_2 = -\frac{\partial \vec{V}_g}{\partial y} \cdot \nabla \left( -\frac{\partial \phi}{\partial p} \right).$$

Finally, taking  $\partial/\partial x$  of (6.38) and adding it to  $\partial/\partial y$  of (6.39) produces

$$-2 \left( \frac{\partial Q_1}{\partial x} + \frac{\partial Q_2}{\partial y} \right) = \sigma \left( \frac{\partial^2 \omega}{\partial x^2} + \frac{\partial^2 \omega}{\partial y^2} \right) - f_0^2 \frac{\partial}{\partial p} \left( \frac{\partial u_{ag}}{\partial x} + \frac{\partial v_{ag}}{\partial y} \right)$$

which becomes, upon substituting from the continuity equation,

$$-2 \left( \frac{\partial Q_1}{\partial x} + \frac{\partial Q_2}{\partial y} \right) = \sigma \left( \frac{\partial^2 \omega}{\partial x^2} + \frac{\partial^2 \omega}{\partial y^2} \right) + f_0^2 \frac{\partial^2 \omega}{\partial p^2} = \sigma \left( \nabla^2 + \frac{f_0^2}{\sigma} \frac{\partial^2}{\partial p^2} \right) \omega. \quad (6.40)$$

The RHS of (6.40) is identically the 3-D Laplacian operator found on the LHS of the classical quasi-geostrophic omega equation (6.26). The forcing function in this form of the quasi-geostrophic omega equation is given by twice the convergence of a 2-D horizontal vector quantity, the  $\vec{Q}$ -vector, defined as  $\vec{Q} = (Q_1, Q_2)$  or

$$\vec{Q} = \left[ \left( -\frac{\partial \vec{V}_g}{\partial x} \cdot \nabla \left( -\frac{\partial \phi}{\partial p} \right) \right) \hat{i}, \left( -\frac{\partial \vec{V}_g}{\partial y} \cdot \nabla \left( -\frac{\partial \phi}{\partial p} \right) \right) \hat{j} \right]. \quad (6.41)$$

Using the hydrostatic relationship ( $\partial \phi / \partial p = -RT/p$ ) we can rewrite this expression in a more convenient form as

$$\vec{Q} = -\frac{R}{p} \left[ \left( \frac{\partial \vec{V}_g}{\partial x} \cdot \nabla T \right) \hat{i}, \left( \frac{\partial \vec{V}_g}{\partial y} \cdot \nabla T \right) \hat{j} \right]$$

which is easier to employ with real weather maps. Looking again at (6.40), we see that if  $\vec{Q}$  is convergent (divergent) then upward (downward) vertical motion results. Also, note that in deriving (6.40) there was no neglect of the deformation terms as we had been forced to do in prior derivations of an omega equation.

Now let us return to our original example of confluent flow superimposed upon a temperature gradient shown in Figure 6.8. The traditional approximations to the quasi-geostrophic omega equation might not be of much help in diagnosing omega in this environment since vorticity advection is rather difficult to determine here. The

6.4 THE  $\vec{Q}$ -VECTOR

171

completeness of the  $\vec{Q}$ -vector comes at the price of increased complication, however. Therefore, we examine the full expression of the  $\vec{Q}$ -vector in order to determine if a simplification, applicable to the example shown in Figure 6.8, is possible. The full expression of  $\vec{Q}$  is given by

$$\vec{Q} = -\frac{R}{p} \left[ \left( \frac{\partial u_g}{\partial x} \frac{\partial T}{\partial x} + \frac{\partial v_g}{\partial x} \frac{\partial T}{\partial y} \right) \hat{i} + \left( \frac{\partial u_g}{\partial y} \frac{\partial T}{\partial x} + \frac{\partial v_g}{\partial y} \frac{\partial T}{\partial y} \right) \hat{j} \right]. \quad (6.42)$$

But there is no  $\partial T/\partial y$  in Figure 6.8 so, again employing the non-divergence of the geostrophic wind,  $\vec{Q}$  simplifies to

$$\begin{aligned} \vec{Q} &= -\frac{R}{p} \left[ \left( \frac{\partial u_g}{\partial x} \frac{\partial T}{\partial x} \right) \hat{i} + \left( \frac{\partial u_g}{\partial y} \frac{\partial T}{\partial x} \right) \hat{j} \right] = -\frac{R}{p} \left( \frac{\partial T}{\partial x} \right) \left( -\frac{\partial v_g}{\partial y} \hat{i} + \frac{\partial u_g}{\partial y} \hat{j} \right) \\ &= -\frac{R}{p} \left( \frac{\partial T}{\partial x} \right) \left[ \hat{k} \times \frac{\partial \vec{V}_g}{\partial y} \right]. \end{aligned} \quad (6.43)$$

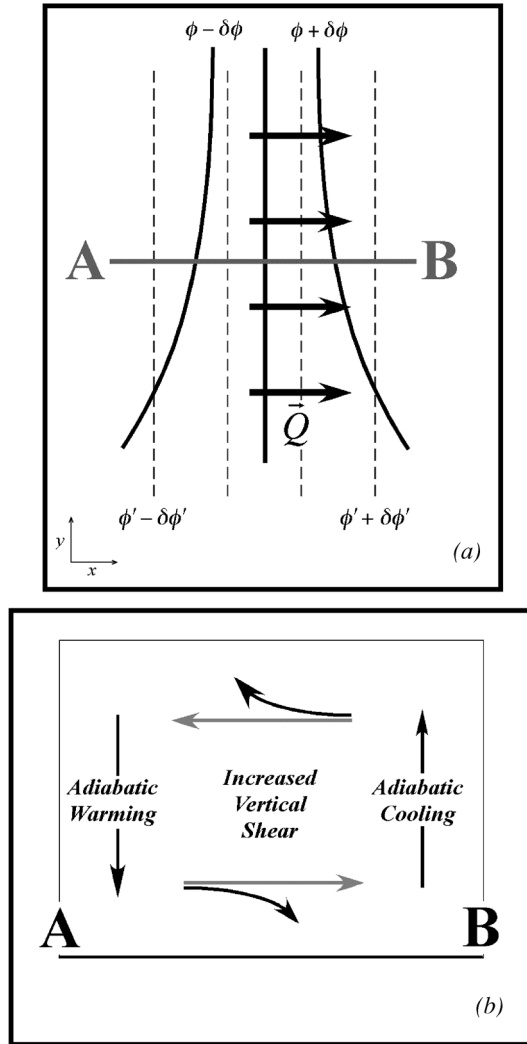
So if one measures the change in the geostrophic wind vector along isotherms (i.e. along the  $y$ -axis), then the direction of the resulting  $\vec{Q}$ -vector is determined as the vertical cross-product of that vector change with its magnitude modulated by the intensity of the  $x$ -direction temperature gradient.

Figure 6.9(a) shows the  $\vec{Q}$ -vectors for the confluent jet entrance of Figure 6.8. This configuration of  $\vec{Q}$ -vectors results in  $\vec{Q}$  convergence in the warm air and  $\vec{Q}$  divergence in the cold air. Consequently, we have diagnosed a thermally direct, secondary, vertical circulation in which the warm air rises and the cold air sinks (Figure 6.9b). Such a secondary ageostrophic circulation achieves two important modifications of the environment. First, adiabatic cooling of the rising warm air and adiabatic warming of the sinking cold air decrease the magnitude of  $\nabla T$ . This exactly counteracts the tendency of the geostrophic temperature advection in the confluent flow! Second, under the influence of the Coriolis force, the horizontal branches of this secondary ageostrophic circulation tend to increase the vertical wind shear – exactly counteracting the tendency of the geostrophic momentum advection in the confluent flow! Thus, the secondary ageostrophic circulation diagnosed with the  $\vec{Q}$ -vectors is precisely that necessary to restore the thermal wind balance in the face of the geostrophic wind's tendency to destroy the balance.

#### 6.4.2 A natural coordinate version of the $\vec{Q}$ -Vector

As we have just seen, the  $\vec{Q}$ -vector is a rather bulky expression but  $-2\nabla \cdot \vec{Q}$  represents a complete form of the forcing in the quasi-geostrophic omega equation. Here we consider an expression for the  $\vec{Q}$ -vector distilled into a natural coordinate version

DIAGNOSIS OF SYNOPTIC-SCALE VERTICAL MOTIONS



**Figure 6.9** (a)  $\vec{Q}$ -vectors for the confluent jet entrance region depicted in Figure 6.8. Vertical cross-section along line A–B is shown in (b). (b) Vertical cross-section along line A–B in (a). Black arrows represent the vertical and horizontal branches of the secondary, ageostrophic circulation associated with the  $\vec{Q}$ -vector distribution in (a). Gray arrows represent the direction of the horizontal branch of the forced circulation before the *Coriolis* force turns in to the right. See text for explanation

that is easily applied to weather maps.<sup>6</sup> We begin with (6.42)

$$\vec{Q} = -\frac{R}{p} \left[ \left( \frac{\partial u_g}{\partial x} \frac{\partial T}{\partial x} + \frac{\partial v_g}{\partial x} \frac{\partial T}{\partial y} \right) \hat{i} + \left( \frac{\partial u_g}{\partial y} \frac{\partial T}{\partial x} + \frac{\partial v_g}{\partial y} \frac{\partial T}{\partial y} \right) \hat{j} \right]$$

<sup>6</sup> This discussion follows work originally done by Sanders and Hoskins (1990).

6.4 THE  $\vec{Q}$ -VECTOR

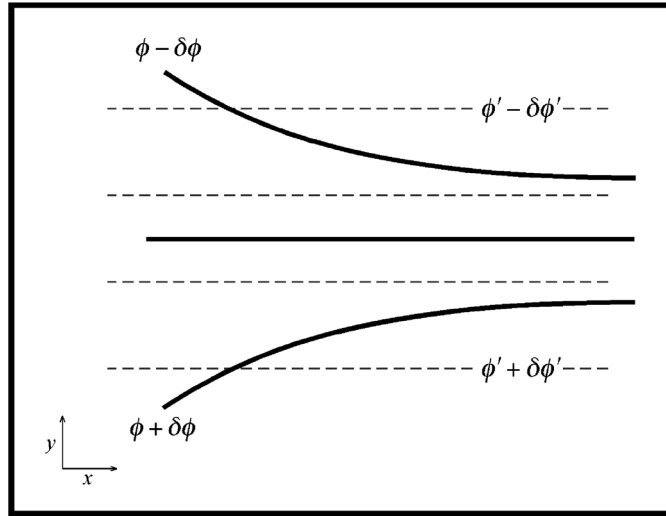


**Figure 6.10** Zonally oriented, confluent jet entrance region in the northern hemisphere. Thick solid lines are 500 hPa geopotential height, dashed lines are 1000–500 hPa thickness. Note that for this flow configuration,  $\partial T/\partial x = 0$

and consider, independently, two extreme examples in which  $\partial T/\partial x = 0$  and  $\partial T/\partial y = 0$ . For the case of  $\partial T/\partial x = 0$  we consider the confluent entrance region of a zonally oriented jet as in Figure 6.10. In such an environment, the above expression reduces to

$$\begin{aligned} \vec{Q} &= -\frac{R}{p} \left( \frac{\partial T}{\partial y} \right) \left[ \frac{\partial v_g}{\partial x} \hat{i} + \frac{\partial v_g}{\partial y} \hat{j} \right] = -\frac{R}{p} \left( \frac{\partial T}{\partial y} \right) \left[ \frac{\partial v_g}{\partial x} \hat{i} - \frac{\partial u_g}{\partial x} \hat{j} \right] \\ &= \frac{R}{p} \left( \frac{\partial T}{\partial y} \right) \left[ \hat{k} \times \frac{\partial \vec{V}_g}{\partial x} \right] \end{aligned}$$

since the geostrophic wind is non-divergent and

$$\frac{\partial v_g}{\partial x} \hat{i} - \frac{\partial u_g}{\partial x} \hat{j} = -\hat{k} \times \frac{\partial \vec{V}_g}{\partial x}.$$

Note that in this example, the  $x$ -axis is in the along-flow direction and the  $y$ -axis is in the across-flow direction, pointing toward colder air.

For the case of  $\partial T/\partial y = 0$ , we appeal to the confluent jet entrance in Figure 6.8 used to illustrate the utility of the  $\vec{Q}$ -vector. In that example, we found that the expression for  $\vec{Q}$  reduced to

$$\vec{Q} = -\frac{R}{p} \left( \frac{\partial T}{\partial x} \right) \left[ \hat{k} \times \frac{\partial \vec{V}_g}{\partial y} \right]$$

and the  $y$ -axis was in the along-flow direction with the  $x$ -axis in the across-flow direction pointing toward warmer air.

Let us now adopt natural coordinates ( $\hat{s}$ ,  $\hat{n}$ ) such that  $\hat{s}$  is directed along the isotherms and  $\hat{n}$  is directed across the isotherms toward warmer air. For the case of  $\partial T/\partial x = 0$  (Figure 6.10) we could say that  $\partial T/\partial y = -|\partial T/\partial n|$  (since  $\partial T/\partial y < 0$ ). Analogously, we could say that  $\partial \vec{V}_g/\partial x = \partial \vec{V}_g/\partial s$  so that our natural coordinate expression for  $\vec{Q}$  would be

$$\vec{Q} = -\frac{R}{p} \left| \frac{\partial T}{\partial n} \right| \left[ \hat{k} \times \frac{\partial \vec{V}_g}{\partial s} \right].$$

For the case of  $\partial T/\partial y = 0$ , we could say that  $\partial T/\partial x = |\partial T/\partial n|$  (since  $\partial T/\partial x > 0$ ). Also, we could say that  $\partial \vec{V}_g/\partial y = \partial \vec{V}_g/\partial s$  so that our natural coordinate expression for  $\vec{Q}$  would be, again,

$$\vec{Q} = -\frac{R}{p} \left| \frac{\partial T}{\partial n} \right| \left[ \hat{k} \times \frac{\partial \vec{V}_g}{\partial s} \right], \tag{6.44}$$

demonstrating that this expression serves as the general natural coordinate expression for  $\vec{Q}$ . In order to apply this expression, we simply denote the vector change in the geostrophic wind along isotherms, take the vertical cross-product of that vector, and flip the resultant direction by 180° (as we must multiply by -1) to determine the direction of  $\vec{Q}$ . The magnitude is modulated by  $|\partial T/\partial n|$ .

Now we examine some examples for which the answers should be fairly familiar. First, let us consider a pattern of sea-level isobars and isotherms for an idealized train of cyclones and anticyclones, illustrated in Figure 6.11. Choosing the middle isotherm as our  $\hat{s}$ -axis, we need only consider the vector change in the geostrophic wind along *that* isotherm. Upon doing so we find that the  $\vec{Q}$ -vectors converge to the east of the sea-level low-pressure center and diverge to its west. Thus, we have diagnosed ascent to the east of the cyclone and descent to the east of the anticyclone.

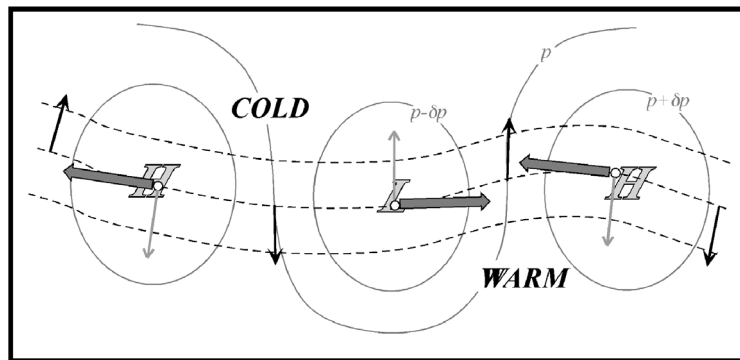


**Figure 6.11** Schematic train of lows and highs in the northern hemisphere. Thin solid lines are sea-level isobars, black dashed lines are 1000–500 hPa thickness, black arrows are surface geostrophic winds, light gray arrows represent  $\partial \vec{V}_g/\partial s$ , and shaded arrows are  $\vec{Q}$ -vectors. See text for explanation

6.4 THE  $\vec{Q}$ -VECTOR

175

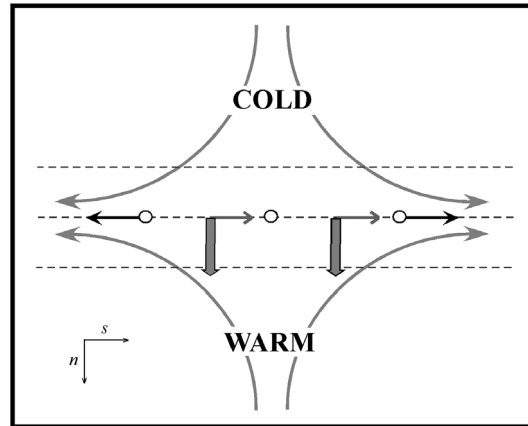


**Figure 6.12** Isotherms in a region of geostrophic deformation. Curved gray arrows are geostrophic streamlines, dashed lines are isotherms or thickness isopleths, black arrows are geostrophic winds at the indicated circles. This gray arrows represent  $\partial \vec{V}_g / \partial s$ , and the shaded gray arrows are the  $\vec{Q}$ -vectors

In this way, the train of cyclones and anticyclones propagates to the east, in the direction of the thermal wind – a result we noted earlier in the chapter.

Next we consider a zonally oriented bundle of isentropes placed in a region of pure geostrophic deformation as illustrated in Figure 6.12. Clearly, this environment would not be easily diagnosed using the traditional form of the quasi-geostrophic omega equation nor any of the approximations to it that we have examined. Picking the middle isotherm as the  $\hat{s}$ -axis, we need only consider the geostrophic wind variation along that isotherm. The resulting  $\vec{Q}$ -vectors are uniformly pointed toward the warm side of the baroclinic zone, indicating rising warm air and sinking cold air – a thermally direct vertical circulation. The differential thermal advection occurring in this deformation zone would tend to bring the isotherms closer together in the horizontal, thereby increasing the thermal wind shear. This same underlying dynamical principle was discussed in reference to Figure 6.4(b). In the next chapter we will more fully discuss the relationship between changes in the temperature gradient and attendant vertical circulations as we discuss frontogenesis. Finally we consider a hypothetical field of uniform geostrophic temperature advection as depicted in Figure 6.13. It is easy to demonstrate that since there is no variation of the geostrophic wind along any isotherm, there is no  $\vec{Q}$ -vector field and, hence, no quasi-geostrophic vertical motion.

We have said that the  $\vec{Q}$ -vector form of the quasi-geostrophic omega equation is a complete form of the forcing. This distinguishes it from the Sutcliffe and Trenberth approximations wherein the deformation terms are neglected. Two reasonable questions to ask at this point in our discussion are (1) where are the deformation terms hiding in the  $\vec{Q}$ -vector forcing, and (2) are they really negligible? The first question is rather academic but the second is crucially important to operational forecasting.

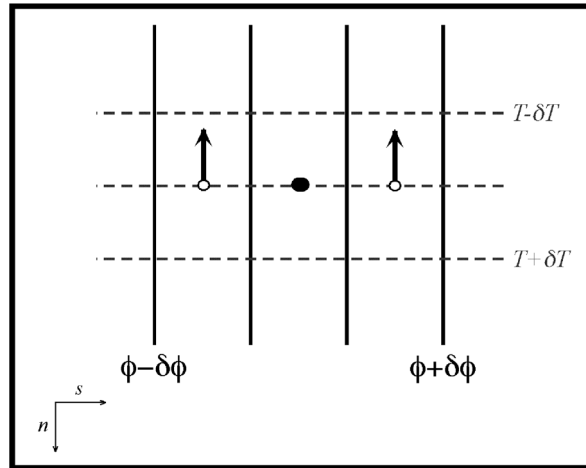


**Figure 6.13** Geopotential heights (thick black lines) and isotherms (dashed lines) in a field of uniform geostrophic warm air advection. Arrows are the geostrophic winds at the indicated points. Since the geostrophic flow is uniform,  $\partial \vec{V}_g / \partial s$  is zero at the black dot and hence there is no  $\vec{Q}$ -vector and no  $\vec{Q}$ -vector divergence

Recall that the forcing for  $\omega$  in the  $\vec{Q}$ -vector form of the quasi-geostrophic omega equation is given by

$$\text{Forcing} = -2\nabla \cdot \vec{Q} = -2 \left( \frac{\partial Q_1}{\partial x} + \frac{\partial Q_2}{\partial y} \right). \quad (6.45)$$

Using (6.42), this can be written as

$$\text{Forcing} = -2 \frac{R}{p} \left[ \frac{\partial}{\partial x} \left( -\frac{\partial \vec{V}_g}{\partial x} \cdot \nabla T \right) + \frac{\partial}{\partial y} \left( -\frac{\partial \vec{V}_g}{\partial y} \cdot \nabla T \right) \right]$$

which expands to four terms after applying the chain rule to yield

$$\begin{aligned} \text{Forcing} = -2 \frac{R}{p} \left\{ \left[ \frac{\partial}{\partial x} \left( -\frac{\partial \vec{V}_g}{\partial x} \right) \cdot \nabla T + \frac{\partial}{\partial y} \left( -\frac{\partial \vec{V}_g}{\partial y} \right) \cdot \nabla T \right] \right. \\ \left. + \left[ -\frac{\partial \vec{V}_g}{\partial x} \cdot \nabla \frac{\partial T}{\partial x} - \frac{\partial \vec{V}_g}{\partial y} \cdot \nabla \frac{\partial T}{\partial y} \right] \right\}. \quad (6.46) \end{aligned}$$

It is left as an exercise to the reader to show that the first square bracketed term on the RHS of (6.46) is exactly equal to the Sutcliffe/Trenberth approximation to the forcing function of the quasi-geostrophic omega equation. Of course, that means that the second square bracketed term on the RHS of (6.46) represents the oft neglected deformation terms. As pointed out previously, these terms will be significant any time a second derivative of temperature is coincident with a first derivative of the geostrophic wind. Frontal zones fit this description but many other characteristic thermal structures observed in mid-latitude cyclones do as well. Figure 6.14

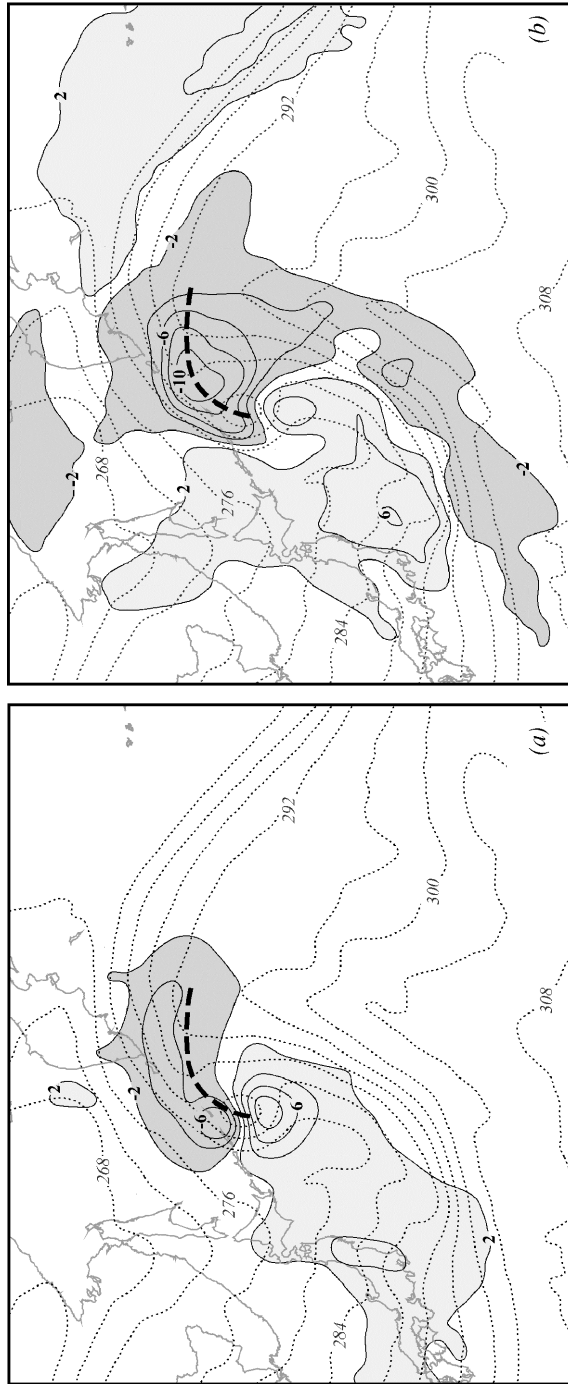


**Figure 6.14** The 700 hPa potential temperature and quasi-geostrophic (QG) vertical motion at 1200 UTC 23 February 2003. Dark (light) shading represents upward (downward) vertical motion labeled in  $\mu\text{ bar s}^{-1}$  ( $\text{dPa s}^{-1}$ ) and contoured every  $-2$  ( $2$ )  $\mu\text{ bar s}^{-1}$  starting at  $-2$  ( $2$ )  $\mu\text{ bar s}^{-1}$ . (a) Sutcliffe/Trenberth approximation to the QG vertical motion. (b) The deformation term contribution to the QG vertical motion. In both panels the thick, dashed line is the axis of the occluded thermal ridge

illustrates the quasi-geostrophic (QG) omega resulting from both the Sutcliffe/Trenberth forcing terms (Figure 6.14a) and the deformation terms (Figure 6.14b) for a modest occluded cyclone. Note that the occluded thermal ridge, a non-frontal thermal structure, is the seat of significant QG vertical motions associated with the deformation terms. This ascent would not be accounted for in the Sutcliffe/Trenberth approximation to the QG omega equation.

### 6.4.3 The along- and across-isentrope components of $\vec{Q}$

A final word concerning the physical meaning of the  $\vec{Q}$ -vector is appropriate before we begin to discuss frontogenesis in Chapter 7. This comment begins by rewriting the hydrostatic equation in the form  $-\partial\phi/\partial p = f\gamma\theta$  where  $\theta$  is the potential temperature and  $\gamma$  is a constant on isobaric surfaces, i.e.

$$\gamma = \frac{R}{fp_0} \left( \frac{p_0}{p} \right)^{c_v/c_p},$$

with  $p_0$  usually taken to be 1000 hPa. Employing this form of the hydrostatic equation allows (6.41) to be rewritten as

$$\vec{Q} = f\gamma \left[ \left( -\frac{\partial \vec{V}_g}{\partial x} \cdot \nabla \theta \right) \hat{i}, \left( -\frac{\partial \vec{V}_g}{\partial y} \cdot \nabla \theta \right) \hat{j} \right]. \quad (6.47)$$

Now let us consider the Lagrangian rate of change of  $\nabla\theta$  following the geostrophic flow, in symbols,

$$\frac{d}{dt_g} \nabla\theta = \left( \frac{\partial}{\partial t} + \vec{V}_g \cdot \nabla \right) \nabla\theta = \left( \frac{\partial}{\partial t} + \vec{V}_g \cdot \nabla \right) \left( \frac{\partial\theta}{\partial x} \hat{i} + \frac{\partial\theta}{\partial y} \hat{j} \right). \quad (6.48)$$

It is left to the reader to show that, under adiabatic conditions,

$$f\gamma \frac{d}{dt_g} \nabla\theta = \vec{Q}.$$

Thus, a profound physical meaning can be ascribed to the  $\vec{Q}$ -vector: that is,  $\vec{Q}$  describes the rate of change of  $\nabla\theta$  following the geostrophic flow. This property of the  $\vec{Q}$ -vector will be exploited in our subsequent discussions of both frontogenesis and cyclogenesis. For now, it is enough that we take advantage of this physical fact to develop additional insight from the  $\vec{Q}$ -vector.

Given that

$$\vec{Q} = f\gamma \frac{d}{dt_g} \nabla\theta,$$

it is useful to consider separately the along- and across-isentrope components of  $\vec{Q}$ , denoted as  $\vec{Q}_s$  and  $\vec{Q}_n$  (where  $\vec{Q} = \vec{Q}_s + \vec{Q}_n$ ), respectively, illustrated in schematic form in Figure 6.15. Before deriving mathematical expressions corresponding to  $\vec{Q}_s$ ,

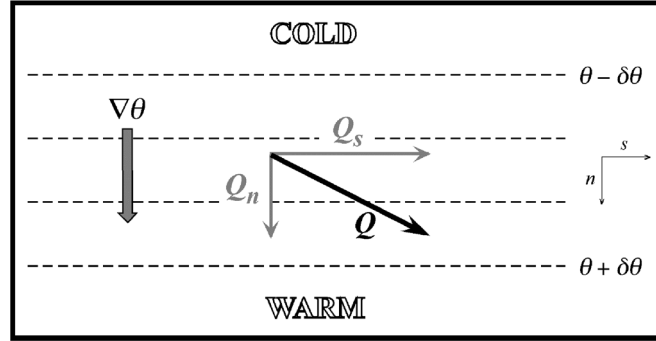


**Figure 6.15** Natural coordinate partition of the  $\vec{Q}$ -vector into its along-isentrope ( $\vec{Q}_s$ ) and across-isentrope ( $\vec{Q}_n$ ) components. See text for explanation

and  $\vec{Q}_n$ , let us consider their respective physical meanings. Noting that the vector  $\nabla\theta$ , like all vectors, has both magnitude and direction, it is clear that  $\vec{Q}_n$ , which is directed along  $\nabla\theta$ , can only affect changes in the *magnitude* of  $\nabla\theta$ . Since  $\vec{Q}_s$  is directed perpendicularly to  $\nabla\theta$  it can only affect changes in the *direction* of  $\nabla\theta$ . Now,  $\vec{Q}_n$  is simply the component of  $\vec{Q}$  along the vector  $\nabla\theta$  and simple vector calculus yields a mathematical expression for  $\vec{Q}_n$  as

$$\vec{Q}_n = \left( \frac{\vec{Q} \cdot \nabla\theta}{|\nabla\theta|} \right) \frac{\nabla\theta}{|\nabla\theta|}. \tag{6.49}$$

Allowing the unit vector in the  $\nabla\theta$  direction ( $\nabla\theta/|\nabla\theta|$ ) to be written as  $\hat{n}$ , and the magnitude of  $\vec{Q}_n$  ( $\vec{Q} \cdot \nabla\theta/|\nabla\theta|$ ) to be written as  $Q_n$ , (6.49) can be rewritten as  $\vec{Q}_n = Q_n \hat{n}$ . Similarly,  $\vec{Q}_s$  is the component of  $\vec{Q}$  along the vector  $\hat{k} \times \nabla\theta$  and so can be written as

$$\vec{Q}_s = \left[ \frac{\vec{Q} \cdot (\hat{k} \times \nabla\theta)}{|\nabla\theta|} \right] \frac{\hat{k} \times \nabla\theta}{|\nabla\theta|} \tag{6.50}$$

where we have taken advantage of the fact that  $|\hat{k} \times \nabla\theta| = |\nabla\theta|$ . Allowing the unit vector in the  $\hat{k} \times \nabla\theta$  direction to be denoted as  $\hat{s}$  and the magnitude of  $\vec{Q}_s$  ( $\vec{Q} \cdot (\hat{k} \times \nabla\theta)/|\nabla\theta|$ ) to be denoted as  $Q_s$ , (6.50) can be written as  $\vec{Q}_s = Q_s \hat{s}$ . Substituting the expressions for both  $\vec{Q}_n$  and  $\vec{Q}_s$ , we can write

$$\vec{Q} = Q_n \hat{n} + Q_s \hat{s}. \tag{6.51}$$

Since the total QG vertical motion is related to  $-2\nabla \cdot \vec{Q}$ , the foregoing partition allows us to see that total as the sum of two orthogonal parts associated with  $-2\nabla \cdot \vec{Q}_n$  and  $-2\nabla \cdot \vec{Q}_s$ , respectively. Given the orientations of  $\vec{Q}_n$  and  $\vec{Q}_s$ , these components of the total vertical motion will be distributed in couplets across the thermal wind (transverse) and along the thermal wind (shearwise), respectively.

It will be shown in the next chapter that the transverse component of the QG omega is directly related to the dynamics of the frontal zones that characterize the

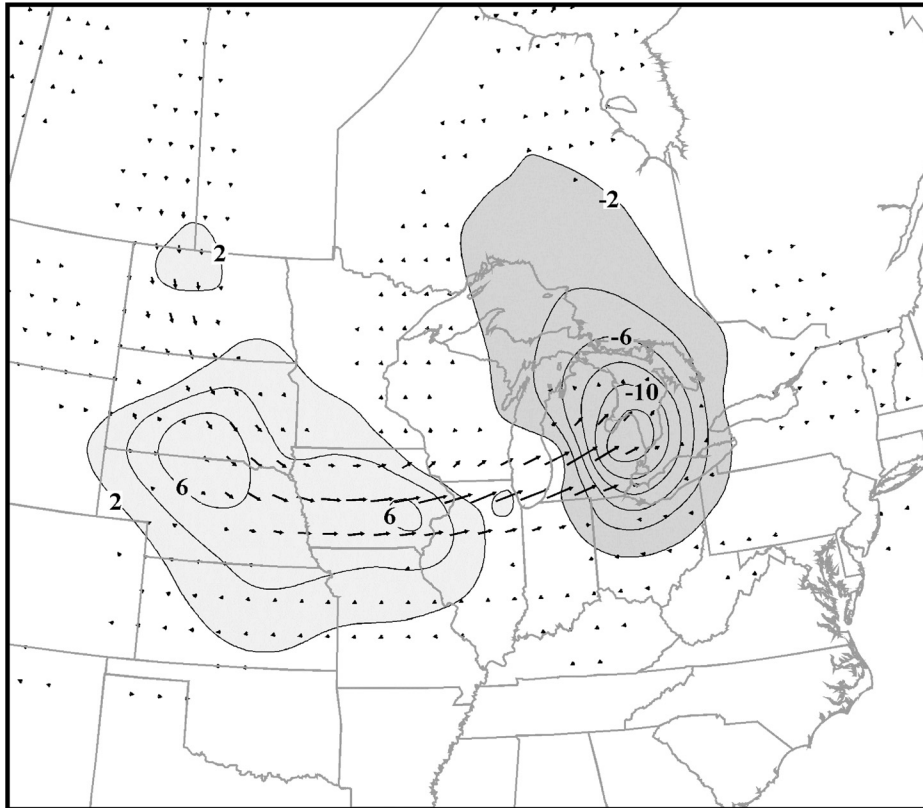


**Figure 6.16** The 700 hPa  $\vec{Q}_{TR}$  vectors (black arrows) and associated QG vertical motion at 0000 UTC 13 November 2003. Vertical motion shown in units of  $\mu \text{ bar s}^{-1}$  ( $\text{dPa s}^{-1}$ ) contoured every  $2\mu \text{ bar s}^{-1}$  with dark shading showing upward vertical motions and light shading showing downward vertical motion

mid-latitude cyclone. Insight into the nature of the shearwise component arises by considering an alternative form of the Trenberth approximation to the QG omega equation in which the thermal wind advection of geostrophic absolute vorticity was the principal forcing mechanism for vertical motions. Starting with (6.32)

$$\sigma \left( \nabla^2 + \frac{f_0^2}{\sigma} \frac{\partial^2}{\partial p^2} \right) \omega \approx 2 \left[ f_0 \frac{\partial \vec{V}_g}{\partial p} \cdot \nabla (\zeta_g + f) \right]$$

and taking advantage of the non-divergence of the geostrophic wind while neglecting the contribution of the planetary vorticity to the geostrophic absolute vorticity, we note that the RHS can be written in a flux divergence form as

$$\sigma \left( \nabla^2 + \frac{f_0^2}{\sigma} \frac{\partial^2}{\partial p^2} \right) \omega \approx 2 \nabla \cdot \left[ f_0 \frac{\partial \vec{V}_g}{\partial p} \zeta_g \right]. \quad (6.52a)$$

But since

$$\frac{\partial \vec{V}_g}{\partial p} = \frac{\hat{k}}{f} \times \nabla \frac{\partial \phi}{\partial p} = -\gamma(\hat{k} \times \nabla \theta),$$

(6.52a) can be rewritten as

$$\sigma \left( \nabla^2 + \frac{f_0^2}{\sigma} \frac{\partial^2}{\partial p^2} \right) \omega \approx -2\nabla \cdot \vec{Q}_{TR} \tag{6.52b}$$

where  $\vec{Q}_{TR} = f_0 \gamma \zeta_g (\hat{k} \times \nabla \theta)$ . Thus, the approximate Trenberth form of the QG omega equation can be written in a form that is identical to the  $\vec{Q}$ -vector form of the full omega equation. Note that the vector  $\vec{Q}_{TR}$  must be everywhere parallel to isentropes and thus  $\vec{Q}_{TR}$  represents at least a portion of  $\vec{Q}_s$ .<sup>7</sup> An illustration of the distribution of  $\vec{Q}_{TR}$  vectors and the associated QG vertical motions from the developing cyclone previously examined in Figure 6.6 are illustrated in Figure 6.16. The distinction between such shearwise and transverse vertical motions will prove valuable when we discuss the process of mid-latitude cyclogenesis in Chapter 8.

### Selected References

- Sutcliffe (1939) offers an illuminating discussion of the ageostrophic wind and its role in producing vertical motions.
- Sutcliffe (1947) describes his famous development theorem.
- Trenberth (1978) describes the cancellation among terms in the traditional QG omega equation.
- Hoskins *et al.* (1978) provide the seminal derivation and discussion of the  $\vec{Q}$ -vector.
- Martin (1998b) examines the appropriateness of neglecting the deformation terms in the QG omega equation from the perspective of the  $\vec{Q}$ -vector.

### Problems

- 6.1. (a) For the mid-latitude, upper tropospheric wave train shown in Figure 6.1A, indicate where the regions of ascent and descent are found. Explain your answer.

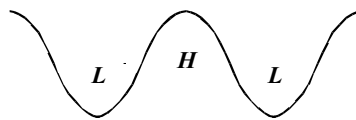


Figure 6.1A

<sup>7</sup> A full description of both the  $\vec{Q}_n$  and  $\vec{Q}_s$  components of the  $\vec{Q}$ -vector, along with their application to the diagnosis of vertical motions in the occluded quadrant of mid-latitude cyclones, is given in Martin (1999).

- (b) The propagating wave train shown in Figure 6.1A will have an associated distribution of height rises and falls as shown in Figure 6.1B. What can be concluded about the relative magnitudes of the isalobaric and inertial advective components of the ageostrophic wind at that level? Explain your answer.

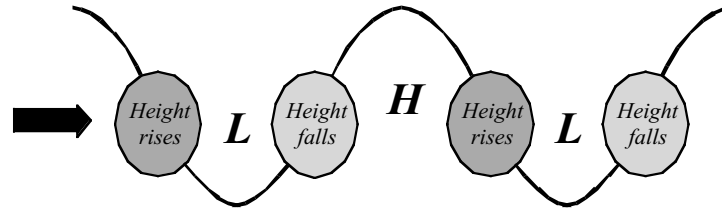


Figure 6.1B

- 6.2. An expansion of the ageostrophic wind consistent with the assumptions of quasi-geostrophic theory can be written as

$$\frac{\hat{k}}{f} \times \frac{d\vec{V}_g}{dt} = \frac{\hat{k}}{f} \times \left( \frac{\partial \vec{V}_g}{\partial t} + \vec{V}_g \cdot \nabla \vec{V}_g \right) = \vec{V}_{ag}.$$

- (a) Given this assumption, show that an expression for the inertial advective component of the ageostrophic wind is given by

$$\vec{V}_{IA} = -\frac{\vec{V}_g \zeta_g}{f}.$$

With simple pictures, show that the distribution of  $\vec{V}_{IA}$  explains:

- (b) the classic four-quadrant vertical motion distribution associated with a straight jet streak, and  
 (c) the distribution of vertical motion associated with an upper tropospheric wave train in the geopotential height field (such as is shown in Figure 6.1A).
- 6.3. This problem refers to the diagnosis of development described by Sutcliffe (1939). The net column ageostrophic wind associated with the Lagrangian rate of change of the shear vector ( $d\vec{V}_s/dt$ ) is always perpendicular to the shear vector itself, which means that any process that changes the shear forces a vertical circulation that is transverse to the shear. Show that the net column ageostrophic wind associated with shearing over the surface wind ( $\vec{V}_s \cdot \nabla \vec{V}_0$ ) is *not* always parallel to the shear vector.
- 6.4. Consider Figure 6.2A which shows 1000–500 hPa thickness contours (dashed lines) along with isopleths of an unknown variable  $Q$  which has the same value at 1000 hPa as it does at 500 hPa.

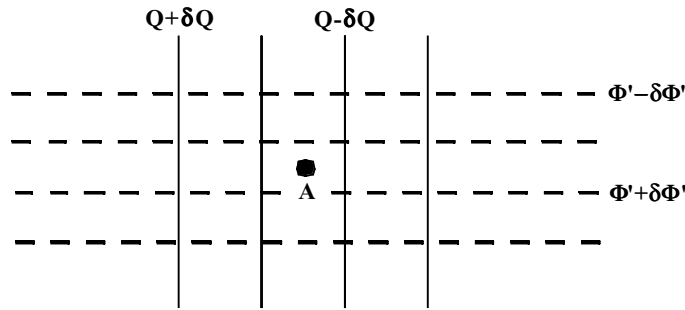


Figure 6.2A

At which level, 1000 or 500 hPa, is the geostrophic advection of  $Q$  at Station A larger? Station A is in the northern hemisphere. Explain your answer. (Hint: use the most basic, *physical* definition of the thermal wind to prove your answer.)

- 6.5. There is partial cancellation between the two separate forcing terms in the traditional quasi-geostrophic omega equation. Describe in words what process is represented by the portion that cancels.
- 6.6. Show that

$$-\frac{\partial\phi}{\partial p} = f\gamma\theta$$

where

$$\gamma = \frac{R}{fp_0} \left(\frac{p_0}{p}\right)^{\frac{c_v}{c_p}}, \quad R + c_v = c_p, \quad \text{and} \quad \theta = T \left(\frac{p_0}{p}\right)^{\frac{R}{c_p}}.$$

- 6.7. Do the *entrance/exit* region circulations associated with a straight jet streak in the southern hemisphere mid-latitudes have the same characteristics as those associated with jet streaks in the northern hemisphere? Explain.
- 6.8. Figure 6.3A illustrates the 700 hPa geopotential height and temperature analysis for a developing mid-latitude cyclone east of the Kamchatka Peninsula in October 2004.
  - (a) Draw  $\vec{Q}$ -vectors at the indicated points using the natural coordinate expression for the  $\vec{Q}$ -vector.
  - (b) Sketch the areas of convergence and divergence of the  $\vec{Q}$ -vectors drawn in (a).
  - (c) Do the areas of convergence and divergence correspond to your intuition about where the air is likely to be rising and sinking in this storm? Explain.

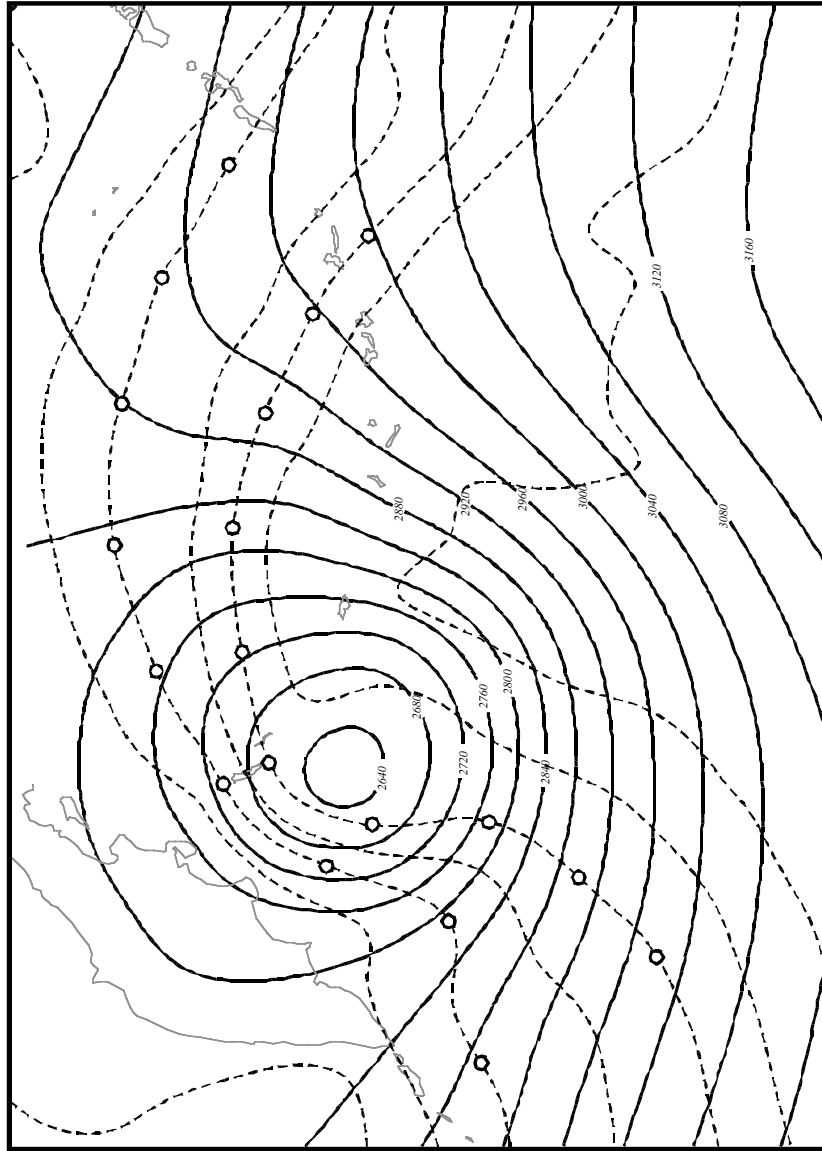


Figure 6.3A

6.9. Figure 6.4A shows the 850 hPa geopotential height (solid lines) and the 1000–850 hPa thickness (dashed lines) in a North Sea ‘reverse shear’ polar low.

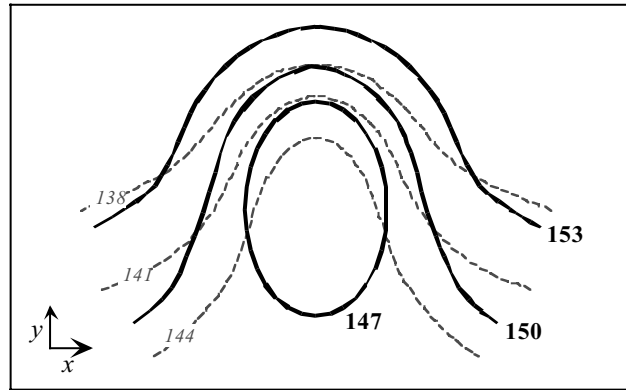


Figure 6.4A

- (a) Indicate with a cross the location of the 850 hPa vorticity maximum.
- (b) Indicate the direction of the 850–1000 hPa thermal wind.
- (c) Use a + and a – to indicate the regions of synoptic-scale upward and downward vertical motions, respectively. Explain your reasoning in terms of the Sutcliffe development theorem.

6.10. Show that

$$\frac{2}{f} \left[ J \left( \frac{\partial \phi}{\partial p}, \nabla^2 \phi \right) + J \left( \frac{\partial \phi}{\partial p}, f f_0 \right) \right] = 2 f_0 \frac{\partial \vec{V}_g}{\partial p} \cdot \nabla (\zeta_g + f).$$

6.11. Demonstrate that the static stability parameter,  $\sigma$ , in the quasi-geostrophic omega equation

$$\sigma = -\frac{1}{\rho \theta} \frac{\partial \theta}{\partial p}$$

can be written in terms of the geopotential,  $\phi$ , as

$$\sigma = \frac{\partial^2 \phi}{\partial p^2} + \frac{c_v}{p c_p} \frac{\partial \phi}{\partial p}.$$

6.12. Prove that, for adiabatic flow,

$$\vec{Q} = f \gamma \frac{d}{dt_g} \nabla \theta$$

where

$$\frac{d}{dt_g} = \frac{\partial}{\partial t_g} + \vec{V}_g \cdot \nabla.$$

186

DIAGNOSIS OF SYNOPTIC-SCALE VERTICAL MOTIONS

- 6.13. Given that  $Q = Q_n \hat{n} + Q_s \hat{s}$ , do you expect that a component of quasi-geostrophic forcing for ascent in a region can result simply from curvature in the isotherms? Explain.
- 6.14. One of the many physical interpretations of the  $\vec{Q}$ -vector is that  $\vec{Q}$  represents the degree of thermal wind imbalance. Why is this an acceptable statement?

**Solutions**

- 6.4. Advection is larger at 500 hPa.